

Review

# The Reynolds Number: A Journey from Its Origin to Modern Applications

Manuel Saldana <sup>1,2,\*</sup>, Sandra Gallegos <sup>1</sup>, Edelmira Gálvez <sup>3</sup>, Jonathan Castillo <sup>4</sup>, Eleazar Salinas-Rodríguez <sup>5</sup>, Eduardo Cerecedo-Sáenz <sup>5</sup>, Juan Hernández-Ávila <sup>5</sup>, Alessandro Navarra <sup>6</sup> and Norman Toro <sup>1</sup>

<sup>1</sup> Faculty of Engineering and Architecture, Universidad Arturo Prat, Iquique 1110939, Chile; chichined@gmail.com (S.G.); notoro@unap.cl (N.T.)

<sup>2</sup> Departamento de Ingeniería Química y Procesos de Minerales, Universidad de Antofagasta, Antofagasta 1270300, Chile

<sup>3</sup> Departamento de Ingeniería Metalúrgica y Minas, Universidad Católica del Norte, Antofagasta 1270709, Chile; egalvez@ucn.cl

<sup>4</sup> Departamento de Ingeniería en Metalurgia, Universidad de Atacama, Copiapo 1531772, Chile; jonathan.castillo@uda.cl

<sup>5</sup> Academic Area of Earth Sciences and Materials, Institute of Basic Sciences and Engineering, Autonomous University of the State of Hidalgo, Pachuca 42184, Mexico; salinasr@uaeh.edu.mx (E.S.-R.); eduardoc@uaeh.edu.mx (E.C.-S.); herjuan@uaeh.edu.mx (J.H.-Á.)

<sup>6</sup> Department of Mining and Materials Engineering, McGill University, 3610 University Street, Montreal, QC H3A 0C5, Canada; alessandro.navarra@mcgill.ca

\* Correspondence: masaldana@unap.cl; Tel.: +56-9-5383-4174

**Abstract:** The Reynolds number (Re), introduced in the late 19th century, has become a fundamental parameter in a lot of scientific fields—the main one being fluid mechanics—as it allows for the determination of flow characteristics by distinguishing between laminar and turbulent regimes, or some intermediate stage. Reynolds' 1895 paper, which decomposed velocity into average and fluctuating components, laid the foundation for modern turbulence modeling. Since then, the concept has been applied to various fields, including external flows—the science that studies friction—as well as wear, lubrication, and heat transfer. Literature research in recent times has explored new interpretations of Re, and despite its apparent simplicity, the precise prediction of Reynolds numbers remains a computational challenge, especially under conditions such as the study of multiphase flows, non-Newtonian fluids, highly turbulent flow conditions, flows on very small scales or nanofluids, flows with complex geometries, transient or non-stationary flows, and flows of fluids with variable properties. Reynolds' work, which encompasses both scientific and engineering contributions, continues to influence research and applications in fluid dynamics.

**Keywords:** fluid mechanics; laminar and turbulent flows; modeling; multiphase flows; fluid dynamics; nanofluids; flows in complex geometries



**Citation:** Saldana, M.; Gallegos, S.; Gálvez, E.; Castillo, J.; Salinas-Rodríguez, E.; Cerecedo-Sáenz, E.; Hernández-Ávila, J.; Navarra, A.; Toro, N. The Reynolds Number: A Journey from Its Origin to Modern Applications. *Fluids* **2024**, *9*, 299. <https://doi.org/10.3390/fluids9120299>

Academic Editors: D. Andrew S. Rees and Giuliano De Stefano

Received: 3 November 2024

Revised: 9 December 2024

Accepted: 12 December 2024

Published: 16 December 2024



**Copyright:** © 2024 by the authors. Licensee MDPI, Basel, Switzerland. This article is an open access article distributed under the terms and conditions of the Creative Commons Attribution (CC BY) license (<https://creativecommons.org/licenses/by/4.0/>).

## 1. Introduction

The Reynolds number (Re) is a dimensionless number that establishes the relation between inertial and viscous forces [1,2], and thus is essential for flow characterization (laminar, transitional or turbulent) [3]. Although Re has no unique definition and its physical meaning varies depending on the context [1], it has a strong influence in fields such as aerodynamics and aeronautics, particularly in transitional flows, where its effects can be non-monotonic and highly sensitive to several parameters [4]. The scaling behavior of turbulent boundary layers is closely related to the dependencies of Re [5]. Generally, the flow in pipes is laminar when  $Re < 2000$  and turbulent when  $Re > 2000$ –2300, with an intermediate transitional range, but varies depending on the source consulted [6]. Interestingly, Re can be interpreted as a curvature ratio, which potentially offers insights

into the design of high-performance exchangers [7] or can be used to help understand the dynamics of the early universe [8].

The concept has a rich history [9] and is essential in various applications of fluid dynamics, including boundary layer theory [10], microfluidics, or fluid physics at the nanometric scale, where other dimensionless numbers such as the Péclet, capillary, and Knudsen numbers also become important [11], as well as mixing processes, chaotic advection, and turbulence [12]. Understanding  $Re$  and related concepts is fundamental for analyzing complex phenomena on a wide range of scales, from nanoliters to geophysical flows [12,13].

This review attempts to synthesize the state of art on  $Re$ , providing an overview of most relevant findings and highlighting both theoretical innovations and practical applications. The review will also compare the theoretical and experimental approaches that have emerged over time, evaluating their impact and accuracy in different contexts. Another goal is to demonstrate the applicability of  $Re$  in various fields, emphasizing its importance in solving complex problems. Finally, this review aims to offer a solid knowledge base that will be useful for both teaching and scientific dissemination, facilitating the understanding and use of the concept in future research and professional settings.

The organization of the work follows the following sequence: in the historical background, an analysis of the origin of  $Re$  is provided, mentioning the first studies and how the need to define this dimensionless number arose. Then, the definition and theoretical foundations are presented, where the formula for the Reynolds number and its basic applications are exposed. In the classical and modern applications section, studies in laminar and turbulent flows and applications in fields such as mechanical engineering, chemistry, biomedicine, and aeronautics are reviewed, along with recent studies on CFD simulations. In the experimental studies and empirical studies section, experimental studies where  $Re$  is measured or calculated are analyzed and compared with theoretical studies, identifying areas of agreement and discrepancies, in addition to studying how  $Re$  behaves in more complex flows, such as non-Newtonian fluids or multiphase flows. In recent advances and developments, a review of recent studies that expand the use of the Reynolds number in emerging areas, such as nanotechnology, bioengineering, or advanced numerical simulations, is presented along with mentions of innovations in Reynolds number theory and how it has been reinterpreted or refined. Discussions present known limitations and ways to address them, along with controversies and debates regarding them. Finally, the main findings and comments about future research are summarized in the conclusions.

## 2. Historical Background

### 2.1. Origins of Reynolds Number

The Reynolds number, a crucial dimensionless parameter in fluid mechanics, originated from the work of Osborne Reynolds on pipe flow in the late 19th century [9,14]. The concept has been applied to various fluid flow scenarios, from microscopic to macroscopic scales [15]. Reynolds' original paper, which introduced the averaging of flow equations, became fundamental in turbulence modeling [16], although both the definition and physical interpretation may vary depending on the application or source used [2,7]. The need to define the dimensionless Reynolds number arose from a desire to understand and predict the behavior of fluids in different flow situations. Until the end of the 19th century, scientists and engineers realized that the behavior of fluids contained many repeating patterns; however, there was no clear method to provide a relationship between such patterns and their physical characteristics—velocity of fluid, viscosity, object, or conduit dimensions. Transitions between smooth, regular flow—subsequently labeled laminar flow—and chaotic, disordered flow—subsequently called turbulent flow—already existed; however, without a proper mechanism, predicting when these changes would occur was very hard. In 1883, British engineer and physicist Osborne Reynolds performed experiments in which he measured how a fluid (water) moved through a cylindrical tube. Reynolds observed that flow behavior not only depends on fluid velocity, but also on additional factors, such

as density, viscosity, and pipe diameter. This led him to define a combination of these variables to characterize the flow [2].

Reynolds's discovery was essential because it provided a way to characterize and predict the type of flow under different conditions. This allowed researchers to classify flows as laminar or turbulent without having to perform experiments for each specific situation, i.e., this mathematical relationship allowed researchers to describe the behavior of fluids in a wide range of applications.

## 2.2. Concept Evolution

Re has evolved significantly since its inception until today. Originally introduced to explain the transition from laminar to turbulent flow in pipes [17], it has become fundamental to characterize flow behavior [1]. Reynolds' work on velocity decomposition into mean and fluctuating components laid the foundation for turbulence modeling [16], and although its generic definition is given as the relationship between inertial and viscous forces [14], its interpretation varies depending on the flow regime [18]. Recent research has explored novel perspectives, such as a relationship of curvatures in spacetime [7] and their role in the transition to turbulence [15]. Despite its long history dating back to Osborne Reynolds and Theodore von Kármán [9], the concept continues to be refined and applied in various fields of fluid mechanics.

Below is a timeline of Re evolution, highlighting key milestones in its development and significance [3,19,20]:

Before the 19th century—early concepts of fluid mechanics: The first attempts to understand fluid motion were made by Greek, Roman, and Arab scholars. Archimedes, for example, studied buoyancy, but the concept of fluid flow remained largely qualitative. Leonardo da Vinci, on the other hand, created the first sketches and observations of fluid flow patterns, including concepts that nowadays are recognized as turbulence.

1700—development of fluid mechanics: Bernoulli developed fluid mechanics by relating fluid flow with pressure and velocity, while Leonhard Euler developed the basic equations of motion for inviscid fluids, now known as Euler's equations. The limitations of both equations were that they did not take viscosity into account.

1800—introduction of viscosity and laminar flow: Navier introduced the concept of viscosity to fluid flow, improving understanding of how fluid layers resist motion, while Stokes expanded on Navier's equations and derived what are known as the Navier–Stokes equations, which describe how viscous fluids behave under different types of forces. These equations take viscosity into account and form the basis of most modern fluid dynamics studies.

1880s—Osborne Reynolds and the birth of the Reynolds number: Reynolds performed his experiments on fluid flow through pipes, where he observed a transition between laminar (smooth) and turbulent (chaotic) flow, establishing Re, a dimensionless quantity that predicts the onset of turbulence based on the ratio of inertial forces to viscous forces. This formula allowed the universal classification of flow regimes. Reynolds also showed that, at low values (typically below 2000), the flow is laminar, and at high values (above 4000), the flow becomes turbulent, declaring a transition region between these values.

Early 1900s—expansion and application of the Reynolds number: Prandtl introduced the concept of the boundary layer (influenced by Re), which was crucial to understanding how fluids interact with solid surfaces and led to significant advances in aerodynamics. Theodore von Kármán then applied the Reynolds number in the study of vortex shedding behind cylindrical objects, contributing to the body of knowledge in fluid dynamics, and finally, engineers began using Re in the design of aircraft wings, propellers, and ships, and applied it to the study of lift, drag, and fluid resistance.

Mid-20th century—computational fluid dynamics (CFD) and expanded use: After WWII, Re became a fundamental tool in the fields of aerodynamics, hydrodynamics, and industrial fluid systems. Engineers used it in wind tunnel tests and large-scale engineering projects (dams, pipelines, cooling systems, etc.), and with the rise of CFD, Re became

an integral part of the computer simulation and modeling of complex fluid flows, allowing phenomena to be explored in regions where physical experiments were impractical or impossible.

21st century—advanced applications and research: Re still remains a critical factor in advanced research and applications that range from biomedical engineering, where it is applied to model the blood flow in arteries (the variation in Re helping in the prediction of diseases like atherosclerosis), to high-Re experiments in the aerospace industry that enable the design of hypersonic vehicles and improvements in the efficiency of commercial air travel, as well as micro- and nanofluidics, where an extremely low Re characterizes laminar flows in applications related to drug delivery and lab-on-a-chip technologies.

Key developments throughout the timeline: The concept of dimensionless numbers expanded beyond the Reynolds number, giving rise to others such as the Froude, Mach, and Prandtl numbers, each of which serves a unique function in fluid dynamics and related fields. The evolution of Re reflects the growing understanding of fluid mechanics, moving from basic observational studies to a quantitative and predictive tool that supports many of the most advanced scientific and engineering projects in the modern world. Re is key in a variety of engineering and science disciplines, and its relevance varies depending on the field and type of flow being studied.

### 2.3. Bibliometric Analysis

The study of the Reynolds number has experienced significant growth in the last century, reflected in the increase in publications in indexed journals (based on SCOPUS bibliographic references), particularly in the last three decades. Bibliometric analysis indicates that 73.6% are original articles and 24.3% are conference papers (the remaining 2.1% correspond to reviews, reports, books, etc.) (see Figure 1a), focusing mainly on areas such as engineering, physics and astronomy, chemical engineering, mathematics, energy, and materials science (see Figure 1b). This expansion in research has led to a deeper understanding and broader applications of the Reynolds number, from its initial conception by Osborne Reynolds in 1883 to its current use in diverse fields (from the study of fluid flow mechanics in pipes to the study of spacetime curvature). Technological advances in experimental methods and computer simulations have allowed researchers to study more complex flows and transition regimes with greater precision. This is evidenced by the exponential increase in scientific work on the subject (see Figure 1c), extending the applicability of the Reynolds number from classical hydrodynamics to modern aerodynamics, microfluidics, and even the study of astrophysical flows.

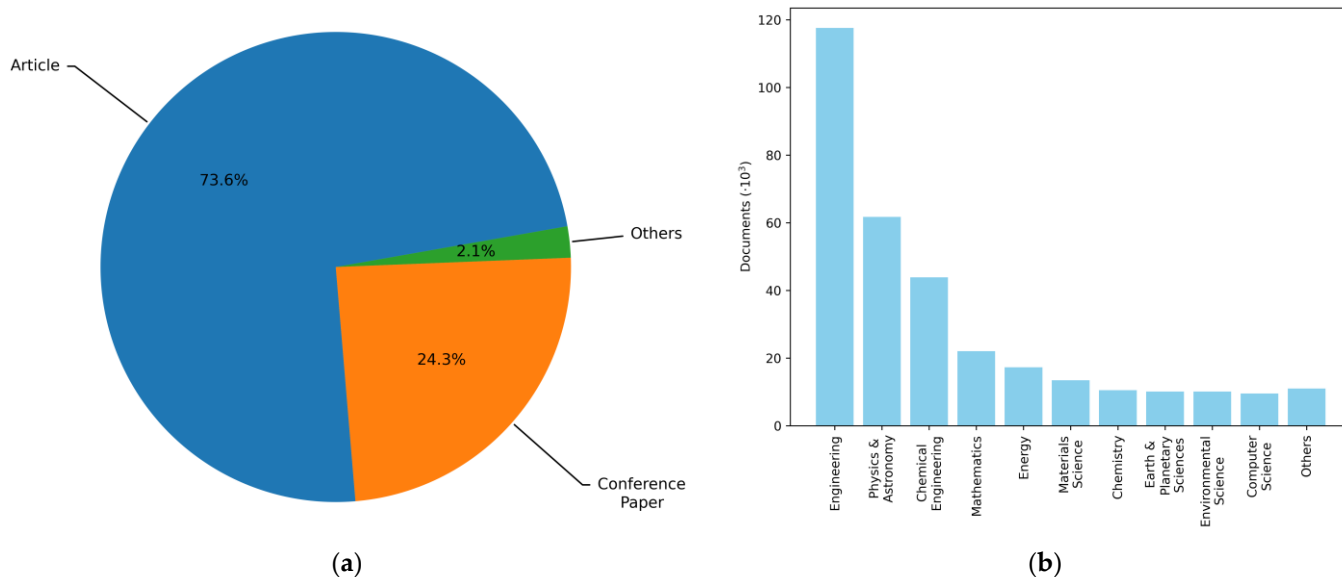
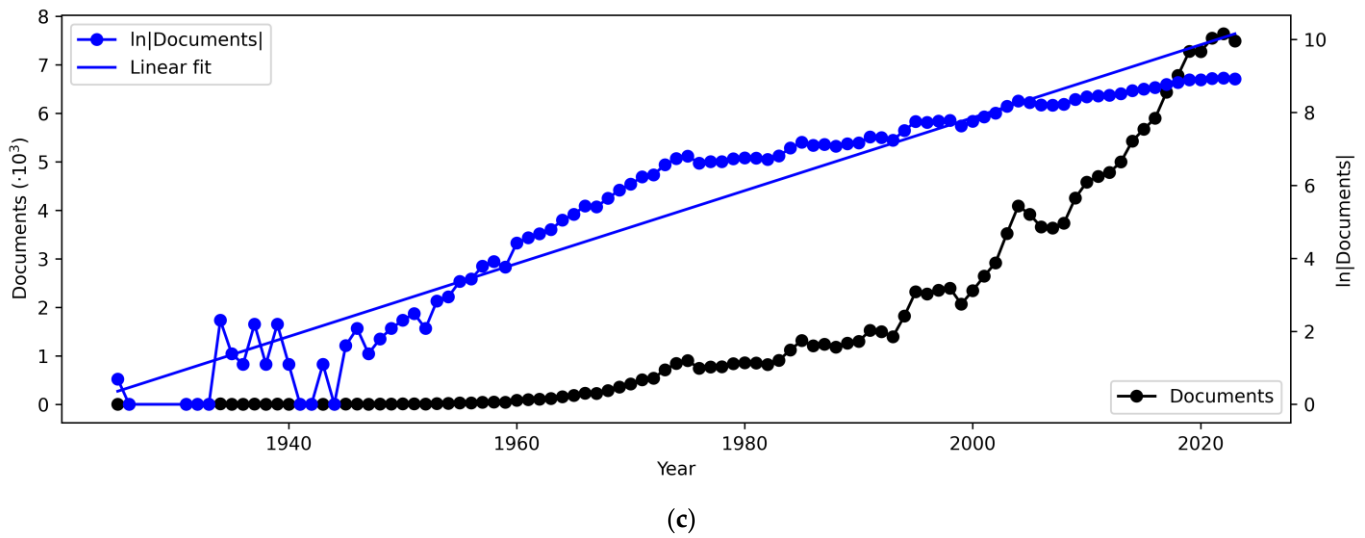


Figure 1. Cont.



**Figure 1.** Distribution of documents by type (a), field of study (b), and temporal variation (c) with respect to the Reynolds number in the SCOPUS bibliographic reference database.

### 3. Definition and Theoretical Foundations

#### 3.1. Mathematical Definition

Re derivation is based on an analysis of the Navier–Stokes equations and the scaling of the characteristic quantities of the flow. The Navier–Stokes equation for an incompressible flow is shown in Equation (1).

$$\rho \left( \frac{\partial \mathbf{u}}{\partial t} + \mathbf{u} \cdot \nabla \mathbf{u} \right) = -\nabla p + \mu \nabla^2 \mathbf{u} \tag{1}$$

where  $\mathbf{u}$  is the velocity vector,  $\rho$  is the fluid density,  $p$  is pressure,  $\mu$  is the dynamic viscosity, and  $\nabla^2 \mathbf{u}$  is a viscous diffusion term. Key terms in Equation (1) are inertial forces  $\left[ \rho \left( \frac{\partial \mathbf{u}}{\partial t} + \mathbf{u} \cdot \nabla \mathbf{u} \right) \right]$  and viscous forces  $[\mu \nabla^2 \mathbf{u}]$ . Then, to analyze these equations in terms of a dimensionless parameter, characteristic flow magnitudes are considered: characteristic length ( $L$ ); characteristic velocity ( $U$ ); characteristic time ( $L/U$ ); and characteristic velocity gradient ( $U/L$ ).

Substituting these scales into the Navier–Stokes terms, the scaling of the inertial forces and the viscous forces are presented in Equations (2) and (3), respectively.

$$\rho \mathbf{u} \cdot \nabla \mathbf{u} \sim \rho \frac{U^2}{L} \tag{2}$$

$$\mu \nabla^2 \mathbf{u} \sim \mu \frac{U}{L^2} \tag{3}$$

Since  $Re$  is defined as the ratio between the inertial and viscous forces, replacing the characteristic scales, its mathematical definition is presented in Equation (4).

$$Re = \frac{\text{inertial forces}}{\text{viscous forces}} = \frac{\rho \frac{U^2}{L}}{\mu \frac{U}{L^2}} = \frac{\rho U L}{\mu} = \frac{\rho \cdot v \cdot L}{\mu} = \frac{v \cdot L}{\nu} \tag{4}$$

where  $\rho$  is fluid density  $\left( \frac{\text{kg}}{\text{m}^3} \right)$ ,  $v = U$  is the characteristic velocity of the flow  $\left( \frac{\text{m}}{\text{s}} \right)$ ,  $L$  is a characteristic length, such as the pipe diameter (m),  $\mu$  is the fluid dynamic viscosity (Pa · s), and  $\nu = \frac{\mu}{\rho}$  is the fluid kinematic viscosity  $\left( \frac{\text{m}^2}{\text{s}} \right)$ .

### 3.2. Physical Interpretation

Reynolds number physical interpretations aim to determine the regime or behavior in which a fluid is found, which can be categorized as: laminar, turbulent, or in transition.

- $Re < 2000$ : indicates laminar flow, where the fluid moves in ordered layers and viscous forces dominate (see Figure 2a).

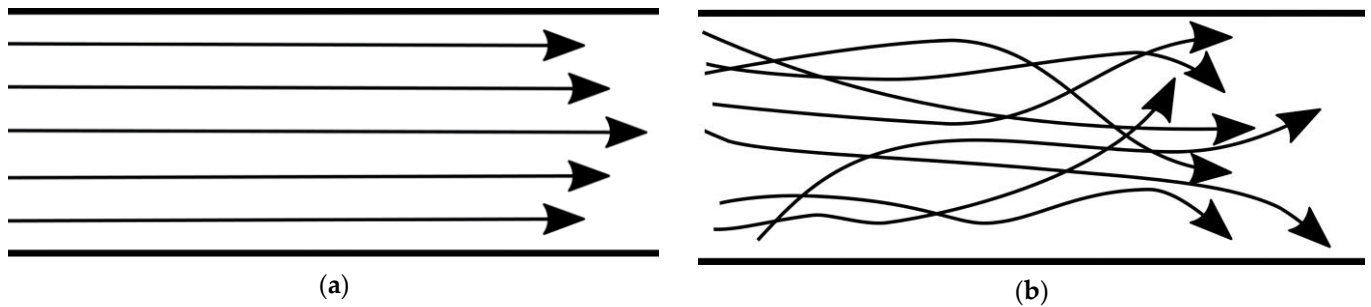


**Figure 2.** Diagrams of laminar (a) and turbulent (b) flow regimes.

- $Re > 4000$ : indicates turbulent flow, where inertial forces predominate and the flow is chaotic (see Figure 2b).
- $2000 < Re < 4000$ : correspond to a transition regime between laminar and turbulent.

The Reynolds number allows for the characterization of flow behavior without having to completely solve the Navier–Stokes equations, acting as a key criterion in the design of experiments and applications in engineering.

### 3.3. Basic Applications

Re has a fundamental role in a variety of applications in hydro- and aeromechanics [21]. Its importance spans aquatic locomotion, biological systems, boundary layer transitions, impact dynamics, engineering systems, and turbulent flow behaviors. Some of the basic applications of the Reynolds number are the study of flow dynamics in pipes, aircraft design, automotive, heat exchangers, industrial mixers, air conditioning flows, hydrodynamics of ships and submarines, and mineral processing. The main basic applications of the Reynolds number are listed below.

#### 3.3.1. Fluid Flow in Pipes

As stated above, the Reynolds number characterizes the flow regime—laminar or turbulent. Therefore, understanding its implications is essential to optimize fluid transport systems in pipes. Laminar versus turbulent flow is understood when  $Re < 2000$ , where the flow is typically laminar, characterized by a smooth and orderly fluid motion, while as  $Re$  increases beyond this threshold, the flow transitions to turbulence, marked by a chaotic and irregular fluid motion [22]. The literature indicates that the transition point can vary depending on factors such as fluid properties and pipe geometry, but  $Re$  remains a fundamental indicator of flow behavior [23]. Additionally, it is noted that, at higher  $Re$ , the azimuthal and streamwise structures of the flow exhibit distinct scale behaviors, influencing the turbulence characteristics and energy distribution within the pipe [23].

The relationship between  $Re$  and velocity fluctuations is significant, and higher  $Re$  leads to greater variation in streamwise and spanwise velocities, affecting overall flow stability and efficiency [24]. Although more basic applications consider the study of the correlation between pressure drops in pipe flows [9], other studies have explored other phenomena, including  $Re$  effects in direct numerical simulations of turbulent flow in pipes and comparison with channels and minimal layers [25], flows through diaphragm orifices in pipes where the orifice functions as a flow meter [26], and flows in pipes with high [27], extreme [28], or variable [29] Reynolds numbers. Additional studies have addressed low- $Re$  flows in helical pipes [30] and the evaluation of laminar flows with high  $Re$ , considering

internal flows, external flows, and flows with special situations such as flow over an obstacle in a wall layer, marginal separation, and unsteady breakup separation [31]. Other studies have examined turbulence bounded by high-Re walls, zero pressure gradient boundary layers, and flows in fully developed pipes and channels [32], along with the scaling properties of turbulent flow in low-Re pipes, where the influence of Re on turbulence statistics such as Re stresses, skewness, and kurtosis is simulated and studied, and where discrepancies in turbulence characteristics at low Re compared to high-Re predictions are also highlighted [33].

Although the transition to turbulence in pipe flow historically occurs at a Reynolds number of around 2000, this limit can even be delayed by up to more than 100,000 under specific conditions where care is taken to inject the liquid into the interior in a uniform manner. In the work developed by Dabiri et al. [34], it is shown that a laboratory jet flow maintains laminar flow beyond a Reynolds number of 116,000, which is confirmed by high-speed videography and flow velocimetry, where the laminar nature of the flow is maintained despite environmental perturbations. The quantified spatial development of the velocity distribution within the jet, which tends to assume a “top-hat” configuration as the distance downstream enlarges, seemingly facilitates the maintenance of laminar flow. These findings imply the presence of a flow regime that is empirically attainable, wherein turbulence may be evaded at an elevated Re.

Finally, instabilities in flow studies arise when a disturbance, however small, grows over time instead of dissipating. These instabilities are usually associated with the physical properties of the flow, the geometry of the system, the boundary conditions, and the problem parameters, such as the Reynolds number. The physical origins of the instabilities can have their genesis in the competition between forces, the interaction with the geometry (where vorticity concentrations or inflection points in the velocity profile are generated, facilitating the amplification of disturbances), and the transition from laminar to turbulent flow.

The stability of a flow can be studied by linear perturbation theory. Assuming that the steady base flow  $U(x, t)$  is perturbed by a small perturbation  $u'(x, t)$ , the total flow is given by Equation (5):

$$u(x, t) = U(x, t) + u'(x, t) \tag{5}$$

where  $u'(x, t) \ll U(x, t)$ . Then, substituting into the Navier–Stokes equations and linearizing (discarding quadratic terms in  $u'$ ), Equation (6) is obtained, where  $\mathcal{L}(U)$  is a linear operator that depends on base flow  $U$ .

$$\frac{\partial u'}{\partial t} = \mathcal{L}(U)u' \tag{6}$$

Assuming modal type solutions as presented in Equation (7), where  $k$  is the wave vector and  $\omega$  is the complex frequency, the stability criterion is given by the following: if  $\text{Im}(\omega) > 0$ , the disturbance grows exponentially ( $e^{\text{Im}(\omega)t}$ ), and the flow is unstable; and if  $\text{Im}(\omega) \leq 0$ , the flow is stable.

$$u'(x, t) = \hat{u}(x)e^{i(kx - \omega t)} \tag{7}$$

### 3.3.2. Aircraft Design

In aeronautics, Re significantly influences the explanation of flow behavior, particularly in transitional flows, affecting vehicle aerodynamics [4]. It significantly affects aircraft design and aerodynamic performance, because as the number increases, the maximum lift coefficient increases, while the minimum drag coefficient decreases [35]. The Reynolds number also affects the pressure distribution, shock wave position, and boundary layer development in supercritical airfoils used in transport aircraft [36,37], and in the case of large aircraft, the effects of Re must be taken into account during design and optimization [37]. Airfoils with a low Reynolds number are crucial for unmanned aerial vehicles

and high-altitude aircraft [38], with airfoil designs varying across Reynolds number ranges, from insect flight to supersonic aircraft. In turbine blade design, on the other hand, the Reynolds number affects flow physics phenomena including boundary layer evolution and wake shedding [39].

Finally, useful tools to investigate the effects of Re are numerical simulations and wind tunnel tests, with computational methods allowing simulations of higher Reynolds numbers comparable to real flight conditions, stressing the models in order to analyze their limits [40,41].

### 3.3.3. Automotive

Re plays a crucial role in automotive aerodynamics and vehicle performance as it significantly influences drag coefficients, whereby higher Re generally leads to lower drag and higher efficiency [42,43]. The effects of Re on vehicle dynamics extend to several aspects including the directionality of motion in self-propelled systems [44] or leveraging the effects of Re to substantially reduce drag, as demonstrated in studies on short blunt bodies [45] and computational models [46]. Re facilitates the study of turbulence control mechanisms, such as: the study of the asymmetric shear layer force, where the use of a small square cylinder to disturb the flow has been tested, determining that it is possible to reduce resistance by up to 8% by improving flow re-insertion and reducing wake asymmetry [47]; the reduction of turbulent resistance by a constant force near the wall [48]; and the use of thermal bands in the direction of the flow to reduce resistance by surface friction, improving the formation of streaks at low speed and suppressing cross-flow fluctuations [49]. These findings have potential applications for automotive design, since they can lead to a more effective management of turbulence and to significant reductions in aerodynamic resistance, improving fuel efficiency and equipment performance.

On the other hand, the effect of turbulence on local drag forces in automotive computational models is significant, as various control strategies can lead to substantial drag reduction. Integrating turbulence management techniques can optimize aerodynamic performance, particularly in complex flow scenarios, so understanding and manipulating Re effects through various design strategies and flow control techniques can lead to significant improvements in automotive performance and efficiency across different transportation domains.

### 3.3.4. Heat Exchangers

The Reynolds number is a key factor influencing heat exchangers performance, affecting both heat transfer and fluid flow characteristics. The reviewed literature indicates that, as the Reynolds number increases, the heat transfer coefficient generally improves while the friction factor decreases [50]. Furthermore, studies on various types of heat exchangers, including shell-and-tube and multi-grid fin designs, have shown that performance can be improved by manipulating geometric parameters and flow conditions [51,52]. Along the same lines, a case study indicates that higher Reynolds numbers improve fluid dynamics, reduce concentration polarization, and enhance membrane performance in electro dialysis desalination [53]. Therefore, in transitional flow regimes, optimal Reynolds numbers can be identified to balance heat transfer and pressure drops [54]. Nanofluids can significantly increase thermal efficiency in heat exchangers [55], and particle size and volume fraction strongly influence their thermophysical properties [56]. The improvement in the thermal efficiency of nanofluids is given by the following conditions: improved thermal conductivity, because nanofluids—fluids containing nanoparticles—have a higher thermal conductivity compared to conventional fluids, allowing for more efficient heat transfer in heat exchangers; the solid volume fraction of nanoparticles significantly affects thermal properties—for example, increasing the graphite concentration in nanofluids improves thermal conductivity, leading to better heat transfer efficiency; the use of nanofluids, especially those based on carbon nanotubes (CNT), has been shown to improve the heat transfer efficiency of plate and plate-fin heat exchangers; and finally, nanofluids also possess unique

thermophysical properties that contribute to their ability to improve the thermohydraulic performance of heat exchangers [55]. Another more recent study corroborates that  $Re$  significantly influences the heat transfer coefficient and the Nusselt number, improving heat transfer and thermal performance in nanofluid applications [22]. Additionally, the stability of nanofluids is crucial, since their instability can reduce system performance considerably [57].

On the other hand, optimal thermodynamic performance of horizontal ground-based heat exchangers in ground-source heat pump systems has been analyzed using various configurations [58], and geothermal heat pump systems, which use the ground as a heat source or sink, have been found to be highly efficient and are becoming popular in heating, ventilation and air conditioning (HVAC). Horizontal circuits are more cost-effective than vertical wells if sufficient land is available, but thermodynamic approaches still need to be improved to evaluate their performance.

### 3.3.5. Industrial Mixers

The Reynolds number plays a crucial role in the performance and efficiency of industrial mixers, influencing flow patterns, mixture quality, and operational parameters and/or responses, so understanding its effects on mixing dynamics can improve the design and application of various mixing technologies. From the literature review, it is evident that experiments show that, as  $Re$  increases, the islands of poor mixing decrease, indicating the directly proportional relationship between mixture quality and mixer speed [59], while simulations of large eddies in stirred tank reactors show that flow structures and vortex formations vary significantly with  $Re$ , affecting the mixing dynamics [60].

Continuing the analysis regarding the flow characteristics, studies on partitioned pipe mixers indicate that the three-dimensionality of the velocity field decreases with increasing  $Re$ , leading to a more chaotic mixing [61], while in the case of studies of more bounded flows, such as jets,  $Re$  is a factor that influences decay rates and turbulence structures in mixing operations [62]. Additionally, high values of  $Re$  can also improve thermal mixing characteristics [63].

### 3.3.6. Air Conditioning Flow

$Re$  plays a crucial role in the dynamics, performance, and efficiency of air conditioning flow and heat transfer as it influences flow characteristics, heat transfer, and sterilization processes, so studying and understanding its effects can lead to optimized designs and improved operating results. In compact heat exchangers, new models have been developed to predict friction factors and heat transfer coefficients over a wide range of Reynolds numbers [64]. For finned tube bundles, correlations between friction factors and Reynolds numbers have been derived to improve the estimation of cooling capacity [65]. In inclined semicircular ducts, a decrease in  $Re$  improves heat transfer rates, particularly in specific orientations, indicating that  $Re$  is a key factor in duct design for HVAC applications [66]. And finally, recent research on microtubes indicates that as  $Re$  increases, both the friction factor and heat transfer efficiency decrease, suggesting that optimal  $Re$  values are critical to maximizing heat transfer in HVAC systems [67].

### 3.3.7. Hydrodynamics of Ships and Submarines

Hydrodynamics of ships and submarines are significantly influenced by  $Re$  [68], affecting drag, wake, maneuvering characteristics, performance, and stability. As aquatic vehicles have improved their speed capabilities, recent research in ship and submarine hydrodynamics has focused on improving numerical simulation methods and understanding complex flow phenomena at high Reynolds numbers, finding applications in the field of technological development including the development of flexible coatings that improve hydrodynamic performance [69]. Therefore, understanding the effects of  $Re$  is essential to optimize the design and operational efficiency of this type of vehicle.

The variation of hydrodynamic coefficients with  $Re$  is significant, particularly at low values. Studies show that using fitted functions instead of constant values yields higher accuracy in estimating these coefficients for underwater vehicles [70], while numerical simulations of submarines, such as the SUBOFF model, reveal that hydrodynamic forces and moments are sensitive to changes in  $Re$ , affecting maneuverability and stability [71]. Research on subsea pipelines, on the other hand, indicates that gas leaks alter wake structures and hydrodynamic forces, and that the interaction of gas bubbles and vortices is strongly dependent on  $Re$  [72]. The behavior of turbulent junction flows, common in subsea appendages, shows that while mean flow characteristics may not vary significantly with  $Re$ , turbulence intensity and heat transfer efficiency do increase, affecting overall performance [73].

Studies have explored the use of dense gases for model testing [74], as the use of highly compressed air and other dense gases allows for full-scale  $Re$  testing of submarines and aircraft, and the implementation of boundary layer transition models for naval applications [75]. Another application of boundary layer transitions studies how the Reynolds number affects the transition of boundary layers over underwater bodies, which impacts design considerations in marine engineering [76].

Advances in computational fluid dynamics (CFD), to be studied in more detail in the next section, have allowed more accurate simulations of turbulent flows around underwater vehicles at high  $Re$  [77], with hybrid URANS/LES methods showing potential for certain applications [78].

### 3.3.8. Mineral Processing

The Reynolds number plays a critical role in mineral processing, influencing fluid behavior and particle transport in a variety of applications, and its impact is seen in processes such as crystallization, mixing, and permeability, which are essential to optimize mineral recovery and product quality. In microfluidic systems, low Reynolds numbers indicate laminar flow, allowing for the precise control of fluids and particles [11]. In solids and gas flow, the Reynolds number affects particle motion and drag in viscous regimes [79]. In mineral suspensions, rheological properties (including  $Re$ ) are influenced by particle concentration and surface chemistry, affecting flow characteristics [80].

$Re$  affects the kinetics of nucleation and crystal growth in membrane crystallization, where higher  $Re$  enhances mass and heat transfer, increasing permeate flux and modifying interfacial supersaturation, which in turn regulates bulk nucleation rates [81]. This relationship allows for refined control over scale-up and crystallization processes. In planetary mixers, on the other hand, increasing  $Re$  correlates with improved mixing quality and experiments show that islands of poor mixing decrease as  $Re$  increases, indicating that higher flow rates enhance material interface interactions [59], which is vital for achieving uniformity in mineral processing. Additionally,  $Re$  also influences apparent permeability in spatially periodic arrays, where higher  $Re$  leads to orientation-dependent permeability changes. This affects fluid flow characteristics essential for efficient mineral extraction [82].

While the Reynolds number is essential to understanding fluid dynamics, its limitations in highly turbulent flows or complex geometries can complicate predictions, requiring advanced modeling techniques to capture the nuances of complex environments, such as near-collisionless plasmas like solar wind [83]. In addition to generating prediction errors, excessive turbulence can also lead to operational challenges, such as increased equipment wear and non-ideal flow patterns, which can affect negatively processing results.

## 4. Classic and Modern Applications

### 4.1. Classical Applications in Hydrodynamics and Aerodynamics

The study of the Reynolds number in hydrodynamics has evolved significantly. In the design of pipelines, a field in which it is required to know a priori whether the flow will be laminar or turbulent,  $Re$  is the criterion par excellence for characterizing flow regimes, as developed by Ryan and Johnson [84], who formulated a criterion to characterize non-

Newtonian fluid regimes. Additionally, Bankston [85] studied the transition of hydrogen and helium gas flow in heated pipelines from turbulent to laminar, concluding that the transition occurs as the heat flow increases and that the transition significantly affected the heat transfer coefficients compared to completely turbulent flow. Spriggs [86] and Barr [87] also analyzed the transition from laminar to turbulent flow, exploring the conditions and implications of this change and providing information on its effects on flow behavior and practical implications for engineering processes.

One of the foundational works on low-Reynolds-number hydrodynamics was presented by Happel and Brenner [88], who explored its applications in several fields, including sedimentation, fluidization, particle size classification, dust and mist collection, filtration, centrifugation, polymer and suspension rheology, flow through porous media, colloidal science, aerosol and hydrosalt technology, lubrication theory, blood flow, Brownian motion, geophysics, and meteorology, among others. Complementing the above, Hinch provides an elementary introduction to the conservation principles governing incompressible fluids, laying the foundation for understanding flow behavior at low Re [89].

Khayat and Eu [90] examined the influence of the Reynolds number on the steady flow properties in cylindrical Couette flow, showing that fluids can behave nearly inviscidly beyond a critical Re. Szwalek and Larsen [91] explored the impact of Re (in turbulent flows) on the hydrodynamic coefficients in vortex-induced forced vibrations, revealing that while certain coefficients showed minimal dependence on Re (the force in phase with velocity, the force in phase with acceleration, and the mean drag coefficient, with Re up to 36,000), trends were observed in specific instability regions, where the hydrodynamic coefficients did not appear to be stable and can be considered to be highly Re dependent. Dewsbury et al. [92], on the other hand, examined the drag coefficient of ascending solid spheres in non-Newtonian fluids over a wide range of Re ( $135 < \text{Re} < 55,000$ ), noting a significant decrease in drag as Reynolds numbers increased, particularly beyond 20,000.

In Meister et al. [93], sensitivity of Re is investigated in the context of the weakly compressible smoothed particle hydrodynamics method, discussing aspects such as physical viscosity and the origin of Couette flow instability, exploring their effects on the convergence properties of the method. Furthermore, a new instability is identified in the flow of pipes with expanding diameters, and both instabilities are observed to occur even at low Re, suggesting that they are caused by high-frequency particle oscillations, unrelated to turbulence. Other applications of Re to hydrodynamics consider measurements of flow dynamics in pipe bends for different regimes [94].

Re plays a crucial role in marine engineering applications, in particular in understanding ship drag, and wake and boundary layer transitions. Studies have shown that Re affects ship drag and wake characteristics, with implications for meshing requirements in computational fluid dynamics (CFD) simulations [95,96], and applications in marine engineering problems [97]. Reynolds-averaged Navier–Stokes (RANS) equations are commonly used to simulate flows at the full scale of Re, which can reach  $10^9$  in naval applications [98]. Several turbulence models have been developed to address the Reynolds number stresses generated by the RANS equations [99]. These models have been applied to analyze marine thrusters [100], submarine models [101], and marine rudders [102]. Recent research has focused on the implementation of boundary layer transition models in CFD codes for naval applications, addressing the challenges of predicting turbulent flows with transition and separation [75]. Hence, understanding hydrodynamic resistances is crucial to optimize ship design and performance [103]. Additionally, other interesting studies include CFD large eddy simulations (LES) focusing on ship hydrodynamics at different Re. These show detailed simulations of turbulent boundary layers and wake characteristics without external turbulence disturbances [104], or, on the other hand, the application of CFD to ship hydrodynamics and naval engineering design [105].

Re also plays a determinant role in aerodynamics and early aviation. It influences laminar flow separation, transitional flow behavior, and the aerodynamic characteristics of airfoils [4], critical for a wide variety of flying vehicles, from birds and bats to human-

powered aircraft and remotely piloted vehicles [106]. At low  $Re$ , typical of small air vehicles and micro air vehicles, laminar flow prevails, affecting airfoil performance and design considerations [107,108]. In airfoil scaling applications, dynamic scaling ensures that flight dynamics are proportionally tuned, and aerodynamic scaling ensures that the scaled aircraft—particularly its airfoil—maintains the same characteristics as the full-sized aircraft, despite differences in  $Re$  caused by changes in length, velocity, and air properties [109]. In contrast, for large air vehicles, the aerodynamics exhibit large Reynolds numbers. Aerodynamic hysteresis, where the lift and drag coefficients become history-dependent near stall angles, is common for round-tip airfoils with low  $Re$  [110]. The Reynolds number affects the maximum lift coefficient, with higher values generally increasing lift and decreasing drag [35,111]. Understanding these effects is critical to designing efficient airfoils for a variety of applications—from insect-sized vehicles to full-scale aircraft—to achieve low drag while maintaining lift performance by optimizing boundary layer development and transition location [112]. Wind tunnel testing must account for Reynolds number effects to accurately predict full-scale aircraft performance [113].

#### 4.2. Classical Applications in Pipe and Canal Engineering

$Re$  plays a crucial role in understanding flow dynamics and sediment transport in sewer systems. It helps determine the flow regimes, from laminar to turbulent, that affect airflow in sewer headspaces [114] and wastewater entrainment [115].  $Re$  is essential for analyzing turbulent coherent structures around sediment reduction plates [116] and formulating mathematical expressions for roughness functions and sediment transport initiation curves [117]. In sedimentation tanks, Reynolds and Froude numbers are used to optimize design and improve efficiency [118]. Hydraulic models can examine stormwater overflow performance at different  $Re$  [119]. Understanding these applications is vital for the effective design and management of sewer systems [120].

Regarding water supply networks,  $Re$  influences flow regimes and pipe friction. It is used to distinguish between laminar, transitional, and turbulent flows [121]. Although for PVC pipes, different equations apply depending on the Reynolds number ranges and pipe diameters [122], the Hazen–Williams equation is commonly used in hydraulic engineering, with limitations based on  $Re$  and pipe size [123].  $Re$  is essential for modeling instantaneous residential water demands and predicting contaminant movement in distribution systems [124], while it is also considered in identifying pipe roughness for both steady-state and dynamic models [125]. Understanding  $Re$  is important to optimize water supply system design [126] and analyze the efficiency, reliability, and vulnerability of a water supply network system [127].

$Re$  also plays a key role in predicting pressure losses in industrial systems. For high  $Re$  piping systems, traditional correlations may be too conservative, requiring new methodologies for more accurate predictions [128]. In duct components, both size and  $Re$  influence pressure loss factors, contrary to previous assumptions [129]. The effects of temperature and pressure on fluid properties must be considered for accurate pressure loss calculations in hydraulic systems [130]. In ventilation systems, the effects of a low Reynolds number are significant, requiring suitable turbulence models for accurate simulations [131], while for non-Newtonian fluids, new relationships between pressure drop and flow rate, as well as Reynolds number expressions, have been derived [132,133].

#### 4.3. Modern Applications in Aeronautical and Automotive Engineering

$Re$  is determinant in the design of wings and fuselages of aircraft and UAVs. Studies have investigated its effects on aerodynamic characteristics over various Reynolds number ranges, from low (200,000–500,000) for UAVs [134] to high (75 million) for large aircraft [135]. Research has shown that increasing  $Re$  (generally) improves aerodynamic performance, with higher maximum lift coefficients and lower minimum drag coefficients [35]. In flying wing designs,  $Re$  affects drag under cruise conditions and influences self-alignment characteristics [136]. Wind tunnel testing and CFD simulations have been employed to study

the effects of Re on several aircraft configurations, including wing-fuselage junctions [137], blended wing bodies [135], and helicopter fuselages [138]. These studies provide valuable data for improving aerodynamic design codes and understanding complex flow phenomena in aircraft design [139].

Regarding aerodynamic optimization of racing cars, Re affects drag, downforce, and overall performance. Studies have shown that variations in Re can significantly affect single-element wings, with up to a 320% difference in downforce observed over a small range of Re [140]. However, multi-element configurations show less sensitivity to Reynolds number changes [140,141]. Optimization techniques have been employed to improve vehicle performance by modifying nose shapes and airfoils [142,143], while wing configuration, including shape and angle, also influences aerodynamic efficiency [144]. Additionally, for Formula One cars, front wing optimization is critical as it contributes approximately 25% of the total downforce. These studies collectively demonstrate the importance of considering Re effects in race car design, from ultra-low Reynolds numbers for micro-air vehicles to higher ranges for full-scale racing cars [42].

Low-Reynolds-number aerodynamics are important for the design and performance of micro aerial vehicles (MAVs), drones, and autonomous underwater vehicles (AUVs) [68,108,145]. These vehicles typically operate in Re ranges below 200,000, where laminar flow prevails and unique aerodynamic challenges arise [145,146]. Factors such as rotor spacing, angle of attack, and turbulence significantly affect the aerodynamic characteristics of these vehicles [68,147]. CFD simulations and experimental studies have revealed the importance of considering transitional flow models in addition to fully turbulent models for accurate performance predictions [148], while biomimetic approaches, inspired by insect flight, offer promising solutions to address the challenges of low-Reynolds-number flight [149]. Understanding these aerodynamic phenomena is essential to improve the efficiency, endurance, and maneuverability of MAVs, drones, and AUVs [146,150].

Reynolds numbers affect significantly the aerodynamic characteristics of supersonic transport vehicles in various flight regimes [151]. In fact, under transonic and subsonic conditions, increasing Reynolds numbers lead to changes in pitching moment, stability, and control effectiveness [152–154], delaying the leading edge separation and pitching moment exit, while improving stabilizer and rudder effectiveness [155]. In supersonic flows, Reynolds number sensitivity affects the formation of shock waves in turbulent shear layers, influencing mixing and combustion processes [156]. The effects are particularly pronounced in transitional flows, where Re variations can cause striking changes in aerodynamic behavior. These phenomena are attributed to changes in boundary layer development, shock wave–boundary layer interactions, and flow separation characteristics [36]. Understanding these effects is critical to accurately predicting flight vehicle performance and optimally designing supersonic transports.

#### *4.4. Modern Applications in Nanotechnology and Microfluidics*

Investigations on the Reynolds number in fluid flows through microchannels reveal complex behavior influenced by channel geometry and flow conditions. Studies show that conventional fluid mechanics theory can often predict flow behavior in microchannels with hydraulic diameters larger than 100  $\mu\text{m}$  [157,158]; however, significant scale effects are observed for channels with heights  $\leq 0.3$  mm [159]. The transition to turbulence in microchannels occurs at lower Reynolds numbers than in macroscale flows, with critical values ranging from 200 to 700 [160] or even as low as 40 [161]. Factors affecting flow through microchannels include channel geometry, surface roughness, viscous dissipation and mainly, and interfaces such as channel walls (that is the reason the critical Re are smaller for small channels) [162], while new approaches to characterize microchannel flows include the introduction of new dimensionless numbers that combine the Reynolds number with geometric parameters [163]. On the other hand, CFD simulations are valuable tools to investigate microchannel flow behavior under various conditions [164].

Microfluidic devices operating at low  $Re$  face challenges in achieving efficient mixing and flow control. Recent studies have shown that turbulence can occur in microfluidics at  $Re \sim 1$  under electrokinetic forcing, exhibiting features such as the Obukhov–Corrsin spectrum [165,166]. To improve mixing efficiency, researchers have explored several designs, including T-shaped micromixers with obstacles and slots [167], magnetic bead-based mixing [168], and flexible thermoplastic film mixers [169]. Flow rectification at low  $Re$  has been achieved using microfluidic bead-based diodes with circular microchannels [170] and single-layer “domino” diodes [171]. The interplay between fluid inertia and elasticity in microfluidic inlet flows has been studied using dilute polymer solutions.

With respect to biomedical engineering, on the other hand, the Reynolds number has important implications, particularly in fluid dynamics and mixing processes. In microfluidic devices, higher  $Re$  results in better mixing and smaller channel widths [172]. For blood flow in cerebral vessels, increasing  $Re$  leads to higher pressure drops and wall shear stress [173].  $Re$  is essential to reconcile discrepancies between Doppler and catheter pressure measurements in aortic stenosis [174,175]. In small centrifugal blood pumps, lower  $Re$  flows deviate from conventional pump affinity laws, necessitating consideration of  $Re$  for accurate scaling [176].  $Re$  also influences cell adhesion in biofouling, with a negative linear correlation observed between adhesion density and the product of the designed roughness index and  $Re$  for both bacterial cells and algal spores [177]. In stenosed artery models, the effect of lesion eccentricity on flow behavior decreases as  $Re$  increases [178]. In the case of intracranial aneurysms, both the  $Re$  and Womersley number affect vortex ring propagation, with the vortex ring location being proportional to  $Re/Wo^2$  [179]. Understanding the effects of  $Re$  is crucial for designing biomedical devices and analyzing biological fluid dynamics [180,181]. The above-cited studies demonstrate the broad applications of  $Re$  in biomedicine, from microscale fluid dynamics to macroscale physiological processes.

Other applications in biology consider the study of hydrodynamic synchronization at low Reynolds numbers, referring to the phenomenon in which fluid interactions synchronize the movements of microscopic objects such as cilia or flagella, which affect bacterial pumping and swimming efficiency [182], and the study of hydrodynamics and hydrodynamic interactions in micron motility, including the propulsion mechanism itself, the synchronized movement of flagella in flagellar bundles, the movement of cilia in cilia arrays, and collective behaviors [183]. Another investigation studies how weakly non-linear self-sustained oscillators synchronize in a fluid environment at low  $Re$ , helping to understand how small-scale physical and biological systems synchronize in fluid environments, which offers insights into natural phenomena such as cell motility or the coordination of microorganisms [184]. In blood flow dynamics, the Reynolds number is vital to model the flow through arteries, where it can be used to predict flow patterns and resistance, which is critical for medical diagnoses and treatments [185].

Research on nanoscale fluid manipulation at low  $Re$  reveals unique phenomena and challenges. Molecular dynamics simulations show deviations from classical Navier–Stokes predictions, particularly near channel walls [186]. Nanoscale surface roughness significantly affects flow patterns, leading to perturbations extending to the channel midplane [187]. Alternating current electric fields can effectively manipulate suspended nanowires despite extremely low  $Re$  [188]. Three-dimensional nanostructures in microfluidic devices improve mixing efficiency at low  $Re$  [189]. The rotational motion of elongated nanoscale objects under external torque can be described analytically and exhibits multiple steady states [190]. Furthermore, computational methods such as molecular dynamics simulations provide valuable insights into fluid behavior at the subcontinuum level [191]. These findings have implications for various applications, including nanorobotics in medical settings [192] and the design of microfluidic devices [11].

#### 4.5. Other Classic and Modern Applications

Additional applications of the Reynolds number in engineering and science can be found in fields such as mechanical engineering, chemical engineering, bridge and dam

design, astrophysics, nanotechnology, renewable energy engineering (wind and offshore turbines), aquatic locomotion, impact dynamics, and aerospace exploration, among others.

In mechanical engineering, applications are found in turbomachines, where  $Re$  affects the overall efficiency and performance [193,194]. In centrifugal compressors,  $Re$  affects the efficiency, head, and flow, requiring correction formulas for accurate performance prediction [195]. In microaxial flow fans, the effects of  $Re$  are not prohibitive, allowing for dimensional analysis and performance scaling [196].  $Re$  also influences wax deposition in oil production systems, affecting flow assurance [197]. RANS modeling is widely used in the industry for CFD simulations, although challenges still exist regarding the reliability of the turbulence model [198]. Considering the above, understanding the effects of  $Re$  is essential to optimize design and performance in various mechanical engineering applications.

From the literature review, a collection of articles can be found where various applications of  $Re$  in chemical engineering are explored. Micromixing technologies are classified based on chemical, biological, and analytical applications [199].  $Re$  effects are studied in turbulent reactive flows, affecting mixing processes and chemical reactions [200,201]. Turbulence fundamentals are applied to reactor modeling and scaling, addressing complex geometries and chemistries [202]. Magnetic resonance is used to study hydrodynamics in chemical engineering systems, including rheology and reactor flows [203]. And finally,  $Re$  correlations are investigated for dense slurry systems with coaxial mixers [204].

Regarding the construction of bridges and dams, or hydraulic structures as a whole, the effects of  $Re$  on the aerodynamics of these structures have been widely studied due to its importance in wind engineering and design. Research shows that  $Re$  can significantly influence aerodynamic force coefficients, Strouhal numbers, and pressure distributions on bridge decks, even those with well-defined edges [205,206]. These effects are particularly pronounced in streamlined and double-box girder bridges [207–209]. High-pressure wind tunnels and CFD have been employed to investigate the effects of  $Re$  over a wide range, from  $10^4$  to  $10^6$  [210,211]. Studies on specific bridges, such as the Great Belt East Bridge, Sutong Bridge, and Stonecutters Bridge, have demonstrated the importance of considering the effects of  $Re$  in the design [205,212]. Furthermore,  $Re$  can affect vortex shedding and the effectiveness of mitigation devices [213]. The above findings underline the need to carefully consider the effects of  $Re$  in bridge design and wind tunnel testing.

Reynolds numbers also play a crucial role in astrophysical turbulence and magnetic reconnection. High  $Re$  in astrophysical environments give rise to turbulent flows [214,215], which affect diverse phenomena from stars to accretion disks. Turbulent reconnection, in which the magnetic field topology changes in turbulent plasmas, is particularly significant in astrophysical environments [216]. This process can be self-driven and has implications for solar flares, gamma-ray bursts, and particle acceleration, while numerical simulations and observational data support turbulent reconnection theories [216,217]. The concept of magnetic flux freezing, fundamental to many plasma theories, is challenged by turbulent reconnection [216]. Scaling laws and similarity criteria have been developed to study astrophysical turbulence in laboratory experiments and simulations, analyzing the relevance of the Reynolds number in astrophysical systems, and studying its role in understanding turbulence and dissipation in high-energy environments [218,219], emphasizing the importance of capturing the full spectral range of high-Reynolds-number flows. It is worth noting that a problem similar to astrophysical magnetic instabilities is that of tokamaks, and that there have been efforts in the magnetic control of this type of plasma through the application of artificial intelligence algorithms [220].

$Re$  influences several aspects of nanoparticle and nanofluid behavior. It affects the manipulation of nanowire lengths in suspension [221] and allows for size control of hybrid lipid-polymer nanoparticles by controlled microvortices [222]. Reynolds number considerations are essential in nanorobotics simulations [223], and it also influences nanodrug delivery in microfluidic channels [224].

Regarding  $Re$  applications in the field of renewable energy engineering,  $Re$  significantly influences the performance and wake characteristics of wind turbines. Studies show

that increasing  $Re$  leads to higher power coefficients, torque coefficients, and optimal tip speed ratios in horizontal-axis wind turbines [225,226]. For vertical-axis turbines, performance becomes independent of  $Re$  at  $Re_D \approx 10^6$  [227]. Low  $Re$  conditions, common in small-scale turbines, can result in reduced efficiency [228]; however, intentional roughness on blade surfaces can improve performance at low  $Re$  [229]. Novel blade designs, such as parabolic-bladed Savonius rotors, show improved aerodynamic performance at low  $Re$  ranges [230]. In the case of semi-passive fin energy harvesters, higher  $Re$  leads to higher energy extraction [231].

$Re$  also plays a determinant role in aquatic locomotion at various scales, helping to analyze the forces acting on aquatic animals such as fish by aiding in understanding swimming efficiency and modes of movement [232]. At low values of  $Re$  ( $<100$ ), viscous forces predominate and organisms use flagellar or ciliary propulsion [233]. At intermediate values of  $Re$  ( $100$ – $10^2$ ), both viscous and inertial forces contribute to thrust and drag [234]. At high values of  $Re$  ( $>10^2$ ), inertial forces predominate and organisms employ wave or pulsed jet propulsion [235,236]. Swimming efficiency and mechanisms vary with  $Re$ , affecting optimal body shapes and locomotion strategies [237]. Scaling laws such as  $Re \sim Sw^\alpha = (\omega AL/\nu)^\alpha$  unify locomotion across taxa [235], and biomimetic studies have explored finning blades and pulsed jet propulsion at different  $Re$ , revealing insights into propulsion efficiency [238,239]. Understanding these principles contributes to the development of biologically inspired aquatic vehicles and to the evolution of swimming adaptations [240].

Regarding the study of impact dynamics, it is noted that events such as droplet impact on solid surfaces, on the other hand, are influenced by several factors, including Reynolds number, surface wettability, and viscosity [241,242]. At high  $Re$ , inertia dominates, generating self-similar pressure fields and propagation patterns, and the impact force initially follows a square root pattern, which matches a known theory on pressure fields, while as the velocity decreases, viscous forces become more important and affect the way droplets deform upon impact [243]. Then, when viscous forces become more significant, this affects the impact force and collision processes [242]. On the other hand, ultra-high velocity impacts introduce compressibility effects, altering flow fields and pressure distributions [244]. The number of fingers in the splash patterns scales with impact Reynolds numbers [245], while for highly viscous and rheologically complex liquids, splashing and rebounding are inhibited at high  $Oh$  numbers [246]. The Reynolds number variation can also be used for the characterization of the in situ modal response of pipe structures [247]. The impact of droplets on spherical targets exhibits distinct temporal phases and is affected by  $Re$  and the target-to-droplet size ratio [248].

$Re$  also plays a critical role in aerospace exploration, influencing several aspects of fluid dynamics and vehicle performance. Low-Reynolds-number airfoils are important for applications such as micro air vehicles and Mars exploration [249].  $Re$  effects are also critical in the design of turbomachinery for space power units [250] and the ground wind load testing of launch vehicles [251]. The ability to accurately simulate flight Reynolds numbers in wind tunnels is crucial for predicting aerodynamic performance, especially in hypersonic regimes [252]. Understanding  $Re$  effects is essential for designing airfoils and airfoils in a variety of environments from Earth to other planets [253,254].

## 5. Advances and Recent Development

$Re$  has diverse applications in different scientific fields. In biology, it helps to analyze complex biological phenomena [232,255]. In aeronautics, it significantly influences flow behavior, particularly in transitional flows [4]. Reynolds number effects are crucial in turbulent wall-bounded flows, as they affect the amounts of mean and statistical turbulence [256]. In superfluid physics, liquid helium wind tunnels can reach exceptionally high Reynolds numbers [257]. In the case of lipid vesicles, increasing Reynolds numbers alter their dynamics in shear flow [258]. New applications include the relationship between the Reynolds number and spacetime curvature [7] and the use of deep reinforcement learning

for flow control in different Reynolds number regimes [259]. Understanding the effects of the Reynolds number is essential for accurate flow prediction and control, especially in external flows with low Reynolds numbers [260].

More recent studies explore new applications of  $Re$  in several fields. In aerodynamics, studies investigate its effects on bionic flaps [261] and surface pattern fabrics for noise and drag reduction [262]. In fluid mechanics,  $Re$  is applied to characterize drilling fluid flow regimes [263] and define the local Reynolds number for CFD simulations [264]. The concept extends to finance, where it is used to identify explosive behavior in stock indices [265] and as a volatility indicator in stochastic time series [266]. In automotive engineering,  $Re$  effects are optimized to reduce aerodynamic drag and improve performance [42]. The study of micropolar nanofluids shows that  $Re$  affects velocity profiles and thermal properties, which is crucial for applications such as drug delivery and blood flow [185]. Variations in  $Re$  affect shock wave interactions in turbulent boundary layers, thereby affecting flow separation and pressure fluctuations, which are critical for aerospace applications [267]. These diverse applications demonstrate the versatility and importance of  $Re$  for understanding complex systems across multiple disciplines.

$Re$  has been widely studied since its original formulation, but in recent decades there have been significant theoretical advances and reinterpretations that have refined its understanding and applications in various areas of science and engineering. Some of the most notable advances are presented below:

1. **Interpretations in Turbulent Flows:** New research has refined how turbulence scales are scaled under high turbulence conditions [268], numerical simulations and experiments have been improved to capture the fine structures of turbulence [269,270], and the use of techniques such as large-scale turbulence and Navier–Stokes direct simulations has allowed for a better understanding of transitions [271,272]. Additionally, subgrid models [273,274] and large eddy simulations (LES) [275] have allowed for a more accurate description of meso- and micro-level flows, improving prediction in aerospace, marine, and meteorological applications.
2. **Non-Newtonian Flows and Complex Fluids:** The Reynolds number has been formulated and generalized for non-Newtonian fluids, such as polymers and gels, because they exhibit non-linear viscosity behaviors [276]. This has allowed for better predictions in fields such as bioengineering [277]. Additionally, some rheological phenomena that occur at a low Reynolds number in a viscoelastic fluid have not been described entirely; for example, the elusive vortices produced by a rotating sphere in a viscoelastic fluid at a low Reynolds number described firstly by Giesekus [278], and later studied numerically by Garduño et al. [279,280].
3. **Microfluidics and Nanofluidics:** Microfluidics and nanofluidics developments have required reinterpretations of  $Re$  for flows at these scales, where surface effects, surface tension, and intermolecular forces dominate over inertial and viscous forces. A new theory that incorporates corrections for flows in geometric confinements at nanometer and micrometer scales has been developed, where  $Re$  tends to be extremely low [281].
4. **Multiscale Applications:** With the rise of multiscale simulations, which attempt to integrate fluid behaviors on scales ranging from molecular to macroscopic, the Reynolds number has been refined to account for effects at multiple levels [282–284].
5. **New Interpretations in Biological and Natural Systems:** Advances have been made in the interpretation of  $Re$  in biological and natural systems. In biological systems, such as insect flight or the movement of microorganisms,  $Re$  is low, meaning that viscous forces predominate [255]. In geophysical flows, such as oceanic or atmospheric flows, the Reynolds number is extremely high, leading to turbulent behavior on large scales [285].
6. **Reynolds Number Corrections for Extreme Conditions:** In the study of flows under extreme conditions, such as high pressure or temperature, or in environments with fluids with exotic properties, work has been done on adjustments to the Reynolds number. To study the fluid dynamics in planetary atmospheres [286], such as those of

Mars or Venus [287], corrections to  $Re$  have been proposed that take into account the low density or viscous properties of the gases present. In fluids under extremely low temperatures, such as superfluids [288–290], the Reynolds number has been modified to reflect quantum effects in fluid dynamics [291].

Recent additional theoretical advances on  $Re$  have explored its importance at various scales and contexts. At high Reynolds numbers, challenges remain in understanding wall-bounded turbulent flows, including the extent of the logarithmic overlay layer and the universality of model parameters [292]. Theoretical estimates of critical  $Re$  have been derived using stochastic equations [293], and new models have been developed to estimate the effects of surface geometry on laminar boundary layers [294]. Researchers have also proposed redefining Reynolds number based on the interplay between macroscopic and microscopic phenomena, potentially offering new insights into turbulence [15].

Research on extreme  $Re$  flows has focused on understanding the scaling laws, coherent structures, and modeling techniques that characterize these turbulent systems. These studies have revealed new insights into the behavior of turbulent flows at high  $Re$ , particularly in terms of mean velocity profiles, friction factors, and the role of coherent structures.

At extreme  $Re$ , the mean velocity profile (MVP) of turbulent pipe and channel flows transitions to new scaling laws. This transition is characterized by complete similarity asymptotics in bulk coordinates and incomplete similarity asymptotics in inner coordinates. A multiscale polynomial model has been proposed to approximate the MVP, providing excellent agreement with experimental data in both bulk and inner coordinates [295]. A novel power-law scaling for the friction factor in extreme  $Re$  pipe flows has been identified by Anbarlooei et al. [296]. This scaling is based on the behavior of coherent structures that dominate momentum exchange in meso-layer regions. This new scaling law aligns well with experimental data from facilities like the Princeton Superpipe, suggesting a shift in the mechanism of turbulent momentum transfer at these high  $Re$  [296]. Studies on extreme turbulent circulation events have also highlighted the role of multifractality breaking in turbulent intermittency. This concept helps describe the asymptotic form of circulation probability distribution functions (cPDFs) [297]. Exact coherent structures (ECS) have been shown to play a fundamental role in transitional and turbulent wall flows, with new insights into their interactions and sustainment mechanisms at high Reynolds numbers [298]. Finally, advances in mathematical methods and computational capacity are paving the way for high-fidelity models of wall turbulence at large  $Re$ . These models aim to predict flow properties accurately while capturing the underlying physics based on the Navier–Stokes equations [299].

Research by Chen and Sreenivasan [24] indicates that at high  $Re$ , a plateau emerges in the velocity fluctuation variations, suggesting a decoupling of  $Re$  effects from wall normal profiles. This finding improves the understanding of turbulence dynamics in channel and pipe flows. In shock wave interactions, Laguarda et al. [300] demonstrate that while the mean flow characteristics remain stable across varying  $Re$ , the dynamics of velocity statistics change significantly, indicating a complex relationship between  $Re$  and flow behavior. Ashoor et al. [301] explore  $Re$  in microvasculature, revealing its role in diagnosing vascular conditions.

Another work of interest was developed by Martínez et al. [302], whose study illustrates how microscopic systems can operate similarly to macroscopic engines while also presenting unique challenges and opportunities due to random (or stochastic) thermal fluctuations. In the work of Martínez et al., the empirical realization of a Carnot engine utilizing a single optically confined Brownian particle as its working medium is delineated, offering an extensive investigation into the energetics of the engine and scrutinizing the fluctuations associated with finite-time efficiency, thereby demonstrating that the Carnot limit may be surpassed with a limited number of non-equilibrium cycles. Mirroring its macroscopic equivalent, the energetics of the proposed Carnot apparatus reveals fundamental characteristics that one would anticipate to manifest in any microscopic energy transducer operating with thermal reservoirs at disparate temperatures.

Future perspectives on Re encompass its implications in various fluid dynamics contexts, particularly in biomedical and turbulence applications, highlighting its pivotal role in fluid dynamics at various scales. Recent studies highlight the nuanced behavior of Re in wall turbulence fluctuations and its diagnostic potential in microvasculature. At low Re, airfoil designs are being developed for planetary exploration [303], while high Re flows present challenges in mixing and turbulent simulation [304]. The RANS approach remains relevant for industrial applications, and potential hybrid RANS/LES strategies are emerging [305]. The criticality of the Reynolds number in dynamic testing requires analytical extrapolation tools to make accurate full-scale predictions [306]. Studies on turbulent boundary layers reveal complex scale behaviors and internal hierarchies of motions [5,299]. Advanced mathematical methods and computational capabilities are enabling the development of high-fidelity models based on Navier–Stokes equations [299]. Interestingly, Re has been conceptualized as a curvature ratio, which could inform heat exchanger design and link hydrodynamics to gravity theory [7].

Additionally, some researchers argue that the traditional focus on Re may overlook other critical parameters that influence flow behavior, suggesting the need for a broader framework in fluid dynamics studies [14,15,88,307,308].

## 6. Discussions

The Reynolds number plays a crucial role in fluid dynamics and aeronautics, influencing flow behavior at various scales. Although it is very useful in several scientific fields, it has some limitations that must be taken into account when using it: model simplification—assuming laminarity or turbulence depending on a critical value, instead of a gradual multifactorial behavior; application in non-homogeneous media, such as in fluids with suspended particles or in porous media, where Re may not be suitable since it does not consider interactions with particles or effects of the medium; evaluation in complex or unconventional geometric conditions, where Re may not provide an accurate representation of the flow behavior dynamics; validity ranges limited to ideal flows, which implies an impossibility to describe flows with forces dominated by electromagnetic effects or non-viscous effects; limitations associated with non-Newtonian fluids, whose viscosity varies with the deformation rate; and limitations related to scales, where the effects of interactions at the molecular level can exceed predictions based on Re, making it inaccurate in these contexts.

Limitations such as low-Reynolds-number phenomena require specialized turbulence models to accurately predict near-wall structures [309]. Limitations in velocity distribution calculations arise at high Re, particularly above 100,000 [310], while scale effects in physical modeling of free surface flows can be minimized by respecting Reynolds and Weber number constraints [311]. High-Reynolds-number flows present challenges for CFD, especially in predicting flow over rough surfaces [312]. Airfoil design, on the other hand, is significantly affected by scale effects, characterized by the chord Reynolds number [106]. The concepts of self-similarity and Reynolds number invariance can help to exclude significant scale effects in Froude modeling [313], and the transition behavior varies widely over Reynolds number ranges, complicating aerodynamic predictions for complex configurations [4].

There are several topics of discussion regarding the interpretation and use of Re to determine the critical value for the transition between laminar and turbulent flows, with several studies that propose slightly different values [314]. There is also debate about the applicability and usefulness of Re in more complex flows than the ideal cases of pipes or flat plates [291]. The interpretation and use of Re in non-Newtonian fluids has also been the subject of debate, since the viscosity is not constant (conventional Re assumption) [315]. There are discussions about the limitations of using the Reynolds number to predict complete similarity between flows at different scales [316]. In the emerging field of microfluidics or nanofluidics, there are debates about how to define and apply the Reynolds number at very small scales [11]. The application of Re in multiphase flows is an active research area with different approaches proposed [317]. There are also

debates on how to interpret and use the Reynolds number in high-velocity compressible flows [318].

Regarding future developments, some of the main research approaches and directions consider applications in complex and multiphysical flows, where the extension or applicability of  $Re$  to more complex systems involving multiple physical phenomena is studied [319], or applications to microfluidics and nanofluidics, where the behavior of fluids at very small scales is studied [320]. For applications to non-Newtonian fluids and complex flows, new approaches are being developed to apply the Reynolds number concept [321], while for applications to turbulence and transition, a detailed understanding of the transition to turbulence and the behavior at very high Reynolds numbers is sought [322]. For applications to advanced numerical simulations, advances in computational capabilities are applied to develop more detailed simulations of high-Reynolds-number flows [323]. New models and approaches are being developed to apply  $Re$  in multiphase flows [324].  $Re$  also has applications in the biomedical industry, such as the in study of blood flow [325]. It can also be applied to active fluids and biological systems, such as bacterial suspensions [326], and in advanced experimental methods, where the behavior of flows at extreme  $Re$  or in difficult-to-access conditions is studied [327].

Additional applications of  $Re$  consider its application to the study of renewable energies, as in the design of wind turbines and marine power generators, in the development of hypersonic vehicles and space exploration, or in the research of new materials and their interactions with fluids. In wind energy,  $Re$  is crucial in the design of wind turbines, since it affects the aerodynamics of the blades and the overall efficiency of the system [328,329]. Regarding hydroelectric energy,  $Re$  is fundamental to understand and optimize the flow in water conduction systems and in the design of hydraulic turbines [330]. In the field of tidal energy, it is important in the design of tidal energy devices to maximize the energy extraction efficiency [331]. In the field of solar thermal energy or geothermal systems, in solar concentrating systems, the number is relevant for the design of heat exchangers and heat transfer fluid systems [331,332]. In biomass processing and biofuel production,  $Re$  is relevant for the design of reactors and mixing systems [333]. In the design of devices to harness wave energy,  $Re$  is important to optimize the interaction between the device and the fluid [334]. Finally, in microhydraulics, or small-scale generation systems, Reynolds number is crucial for the design of microturbines and drive systems [335].

Regarding the development of hypersonic vehicles and space exploration,  $Re$  influences aerodynamic design, heat transfer, and other critical aspects. In hypersonic aerodynamics,  $Re$  is fundamental to understand and predict the flow behavior around hypersonic vehicles [336] and is addressed in studies on heat transfer in the atmospheric reentry of space vehicles [337], the design of rockets and launch vehicles, where  $Re$  is crucial to optimize aerodynamics and efficiency [338], and on the aerodynamics of planetary exploration vehicles, where atmospheric conditions are different [339]. In the development of propulsion systems for space travel,  $Re$  is relevant for the design of nozzles and combustion chambers [340]. In hypersonic wind tunnels,  $Re$  is crucial in the design and operation [341]. It is also relevant to the study of the following areas: the fluid–structure interaction of vehicles under hypersonic conditions [342]; the dynamics of rarefied gases, such as the upper layers of the atmosphere and space [343]; the modeling of atmospheric flows on other planets for exploration missions [344]; the design of heat shields to protect vehicles during atmospheric reentry [345]; and finally, magnetohydrodynamics in space propulsion, where the magnetic  $Re$  is relevant in the study of magnetohydrodynamic propulsion for space travel [346].

The Reynolds number has been utilized in research on new materials and their interactions with fluids, which is crucial in the development of advanced materials with specific properties for applications in various areas. In superhydrophobic materials,  $Re$  is crucial to understanding how these materials interact with fluids, especially in relation to friction reduction and self-cleaning [347]. Regarding to the behavior of nanofluids,  $Re$  is especially determinant in applications in heat and energy transfer [348]. To understand the

dynamics of flows through porous media, it is crucial in filtration and energy storage applications [349].  $Re$  is also used for studying the effectiveness of antifouling coatings, used to prevent the accumulation of organisms on submerged surfaces [350], and for studying smart materials that change their properties depending on flow conditions, characterized by a certain  $Re$  [351].  $Re$  is used in research on materials that reduce drag in fluids at high  $Re$  for applications in energy efficiency [352], the study of nanocomposites designed to improve heat transfer in fluid systems [353], the development of materials for biomedical applications [354], the study of the ability of self-cleaning materials to repel contaminants under different flow conditions [355], research on materials that can actively modify flow characteristics at different  $Re$  [356], and the design of materials for efficient  $CO_2$  capture in gas flows [357].

These applications demonstrate the importance of the Reynolds number in various aspects of renewable energy development, hypersonic vehicle development, and space exploration, and its use in research into new materials. Research in areas such as hypersonic or space vehicle development continues to develop, seeking to improve understanding and the ability to design more efficient and safer vehicles and systems for space exploration and hypersonic flight.

## 7. Conclusions

Recent research on the effects of  $Re$  on fluid dynamics has revealed significant trends and discoveries over the last decades. Studies have shown that the influences of the Reynolds number are particularly strong in transitional flows, with a transition occurring over a wide range of values, which is a function of the fluid dynamics under study. Turbulent flows at high  $Re$  exhibit a universal scaling behavior for velocity fluctuations, similar to the scaling of the mean velocity distribution, while the approach for asymptotically high  $Re$  is slow, and the logarithmic law remains fundamental in the description of mean flow. Very large scale motions become increasingly important at higher  $Re$ , interacting with smaller scales near the walls.

The convergence between classical and modern approaches in the study of  $Re$  represents an area of interest in contemporary fluid mechanics, because it combines established theoretical foundations with new technologies and analysis methods. Some key points of this convergence are given by the following conditions: the integration of classical theory and advanced numerical simulations, which enable the validation and extension of classical  $Re$  theories to previously inaccessible regimes; the refinement of the transition to turbulence, which improves understanding of the transition; the extension and adaptation of the classical concept to the application to complex non-Newtonian fluids; the reinterpretation of classical  $Re$  theory to micro- and nanofluidics applications; the development of advanced experimental methods allowing for the validation and refinement of the classical theories; the interdisciplinary applications of the classical  $Re$  concept to modern fields such as bio-fluidics and active matter physics (such as blood flow and locomotion of microorganisms); the refinement of the classical theory and its adaptation to extremely high  $Re$  flows; the application of modern complex systems or system dynamics approaches to gain a better understanding of classical phenomena related to  $Re$ ; the application of classical concepts to modern technologies related to renewable energy development and the environment; the integration of classical theory with modern fluid–structure interaction models; the combination of classical concepts with modern flow control techniques; and the application of modern data analysis and machine learning techniques to extract new insights from classical data. Current trends also include advancements in understanding  $Re$  effects on interface phenomena such as droplet and bubble formation processes, as well as the application of the concepts in large-scale geophysical flows such as ocean and atmospheric currents.

The convergence between classical and modern approaches is leading to a richer and more nuanced understanding of  $Re$  and its role in fluid dynamics, while the integration of classical theories with new technologies or analysis methods is opening the door to new

research and applications, allowing us to address more complex and challenging problems in fluid science and mechanics. The importance of  $Re$  in future research areas in fluid mechanics and related fields lies in its ability to characterize the dynamics of flow behavior and its applicability in a wide range of scales and phenomena. Some areas where  $Re$  will be crucial in future research are listed as follows:

1. Understanding turbulence at very high Reynolds numbers.
2. Advanced microfluidics and nanofluidics: fluid behavior at very small scales, where surface effects dominate.
3. Complex fluids and soft materials: application to non-Newtonian fluids, complex suspensions, and soft materials.
4. Active fluids and active matter: study of systems where particles can self-propel, such as in bacterial suspensions, swarms of robots, or collaborative robotics in fluid environments.
5. Fluid–structure interactions: understanding how flexible structures interact with flows at different  $Re$ , designing more efficient and resilient structures.
6. Multiphase and multiscale flows: application in systems involving multiple phases or scales.
7. Fluids in extreme conditions: fluid behavior under extreme conditions of pressure or temperature, relevant to geophysical and astrophysical applications.
8. Shape optimization and flow control: using  $Re$  in aerodynamic and hydrodynamic shape design and optimization.
9. Flows in biological systems: application in biological systems, from blood flow to locomotion of organisms.
10. Transition to turbulence: a detailed understanding of how and why flows transition from laminar to turbulent.
11. Advanced numerical simulations: development of more advanced numerical methods will allow simulating flows at extreme  $Re$  in more complex geometries.
12. Applications in energy and environment: development of more efficient energy technologies and understanding of environmental phenomena.

Despite the extensive research on  $Re$  developed during the last decades, there are still various gaps in its knowledge and understanding, areas that give important opportunities for future research. The main identified gaps are that the mechanism of when a laminar flow transitions to turbulence at some critical  $Re$  is not fully known, or there is a gap in knowledge regarding how flows behave at extreme  $Re$ , as mentioned for astrophysical and geophysical applications. The applicability of  $Re$  in complex non-Newtonian fluids, such as polymers or concentrated solutions, is still a challenging issue; the interaction between the effects of  $Re$  and compressibility in high-velocity flows is not fully known, and the definition and application of  $Re$  in complex multiphase flows, such as liquid-gas mixtures or particle suspensions, also remains an open question. The applicability of  $Re$  on very small scales, where surface effects dominate, is also not fully known. The application in self-propelled particle systems or active fluids represents an emerging area with a lot of open questions. The understanding of its effect on fluid–structure interactions under unsteady conditions is incomplete, the exact influence of surface roughness at critical  $Re$  and when reaching the transition to turbulence is not fully characterized, the application in complex geometries and how it relates to flow structures is not fully known, and the influence of external fields, such as magnetic or electric fields, on the flow behavior for various  $Re$  is also not known.

**Author Contributions:** Conceptualization, M.S. and N.T.; methodology, M.S., A.N. and N.T.; validation, S.G., E.G., J.C., E.S.-R., E.C.-S. and J.H.-Á.; formal analysis, M.S., S.G., E.G., J.C. and E.S.-R.; investigation, M.S., J.C., E.S.-R., E.C.-S., J.H.-Á., A.N. and N.T.; writing—original draft preparation, M.S.; writing—review and editing, M.S., E.C.-S., J.H.-Á., A.N. and N.T. All authors have read and agreed to the published version of the manuscript.

**Funding:** This research received no external funding.

**Data Availability Statement:** No new data were created or analyzed in this study. Data sharing is not applicable to this article.

**Acknowledgments:** Manuel Saldana acknowledges the infrastructure and support from Doctorado en Ingeniería de Procesos de Minerales at the Universidad de Antofagasta.

**Conflicts of Interest:** The authors declare no conflicts of interest.

## References

1. Uruba, V. Reynolds Number in Laminar Flows and in Turbulence. *AIP Conf. Proc.* **2019**, *2118*, 020003. [[CrossRef](#)]
2. Smith, L.H. Some Comments on Reynolds Number. *J. Eng. Power* **1964**, *86*, 225–226. [[CrossRef](#)]
3. Batchelor, G.K. *An Introduction to Fluid Dynamics*; Cambridge University Press: Cambridge, UK, 2000; ISBN 9780521663960.
4. Bushnell, D.M.; Yip, L.P.; Yao, C.-S.; Lin, J.C.; Lawing, P.L.; Batina, J.T.; Hardin, J.C.; Horvath, T.J.; Fenbert, J.W.; Domack, C.S. *Reynolds Number Influences in Aeronautics*; NTRS—NASA Technical Reports Server: Hampton, VA, USA, 1993.
5. Klewicki, J.C. Reynolds Number Dependence, Scaling, and Dynamics of Turbulent Boundary Layers. *J. Fluids Eng. Trans. ASME* **2010**, *132*, 094001. [[CrossRef](#)]
6. Hillebrandt, W.; Gupta, F. An Introduction to Turbulence. In *Lecture Notes in Physics*; Springer: Berlin/Heidelberg, Germany, 2008; Volume 756, pp. 1–20. [[CrossRef](#)]
7. Delplace, F. Reynolds Number and Spacetime Curvature. *Fluid Mech. Open Access* **2016**, *3*, 1000125. [[CrossRef](#)]
8. Giovannini, M. Reynolds Numbers in the Early Universe. *Phys. Lett. B* **2012**, *711*, 327–331. [[CrossRef](#)]
9. Krause, E. Application of Numerical Techniques in Fluid Mechanics. *Aeronaut. J.* **1974**, *78*, 337–354. [[CrossRef](#)]
10. Gersten, K. Introduction to Boundary-Layer Theory. In *Recent Advances in Boundary Layer Theory*; CISM International Centre for Mechanical Sciences; Springer: Vienna, Austria, 1998; Volume 390, pp. 1–8. ISBN 978-3-7091-2518-2.
11. Squires, T.M.; Quake, S.R. Microfluidics: Fluid Physics at the Nanoliter Scale. *Rev. Mod. Phys.* **2005**, *77*, 977–1026. [[CrossRef](#)]
12. Ottino, J.M. Mixing, Chaotic Advection, and Turbulence. *Annu. Rev. Fluid Mech.* **1990**, *22*, 207–254. [[CrossRef](#)]
13. Faber, T.E.; Lumley, J.L. Fluid Dynamics for Physicists. *Am. J. Phys.* **1996**, *64*, 1214–1215. [[CrossRef](#)]
14. Patel, Y.; Sanyal, A.; Sharma, D.; Rai, S.; Basu, D.; Patel, S.; Jyoti Sen, D. Dimensionless Reynolds Number as a Dimension for Fluid Mechanics in Rheology. *J. Drug Discov. Ther.* **2017**, *5*, 25–30.
15. Bodmann, B.E.J.; Vilhena, M.T.; Zabadal, J.R.; Beck, D. On a New Definition of the Reynolds Number from the Interplay of Macroscopic and Microscopic Phenomenology. In *Integral Methods in Science and Engineering*; Birkhäuser Boston: Boston, MA, USA, 2011; pp. 7–14. [[CrossRef](#)]
16. Launder, B.E. First Steps in Modelling Turbulence and Its Origins: A Commentary on Reynolds (1895) ‘On the Dynamical Theory of Incompressible Viscous Fluids and the Determination of the Criterion’. *Philos. Trans. R. Soc. A Math. Phys. Eng. Sci.* **2015**, *373*, 20140231. [[CrossRef](#)]
17. Kilgore, R.A. Evolution and Development of Cryogenic Wind Tunnels. In Proceedings of the 43rd AIAA Aerospace Sciences Meeting and Exhibit—Meeting Papers, Reno, NV, USA, 10–13 January 2005; pp. 7133–7144. [[CrossRef](#)]
18. Uruba, V. On Reynolds Number Physical Interpretation. *AIP Conf. Proc.* **2018**, *2000*, 020019. [[CrossRef](#)]
19. Rouse, H. The Origins of Fluid Mechanics. *J. Eng. Mech.* **1987**, *113*, 66–71. [[CrossRef](#)]
20. Tokaty, G.A. *A History and Philosophy of Fluid Mechanics*, 1st ed.; Dover: New York, NY, USA, 1994; ISBN 0486681033.
21. Prandtl, L.; Tietjens, O.K.G. *Applied Hydro- and Aeromechanics: Based on Lectures of L. Prandtl*; Dover: New York, NY, USA, 1957; ISBN 9780486603759.
22. Basavaraj, K.; Elangovan, K.; Shankar, S.; Kulkarni, A. Satyanarayan Effects of Reynolds Number on the Volume Concentration of Al<sub>2</sub>O<sub>3</sub> in Ethylene Glycol. *Int. J. Veh. Struct. Syst.* **2023**, *15*, 351–355. [[CrossRef](#)]
23. Zanon, E.S.; Dewidar, Y.; Egbers, C. Reynolds Number Dependence of Azimuthal and Streamwise Pipe Flow Structures. *J. Fluid Mech.* **2023**, *973*, A1. [[CrossRef](#)]
24. Chen, X.; Sreenivasan, K.R. Reynolds Number Asymptotics of Wall-Turbulence Fluctuations. *J. Fluid Mech.* **2023**, *976*, A21. [[CrossRef](#)]
25. Chin, C.; Monty, J.P.; Ooi, A. Reynolds Number Effects in DNS of Pipe Flow and Comparison with Channels and Boundary Layers. *Int. J. Heat Fluid Flow* **2014**, *45*, 33–40. [[CrossRef](#)]
26. Mech, A.M.I.E. Flow through Pipe Orifices at Low Reynolds Numbers. *Proc. R. Soc. Lond. Ser. A Contain. Pap. A Math. Phys. Character* **1930**, *126*, 231–245. [[CrossRef](#)]
27. Zagarola, M.V.; Smits, A.J.; Orszag, S.A.; Yakhot, V. Experiments in High Reynolds Number Turbulent Pipe Flow. In Proceedings of the 34th Aerospace Sciences Meeting and Exhibit, Reno, NV, USA, 15–18 January 1996. [[CrossRef](#)]
28. Hultmark, M.; Vallikivi, M.; Bailey, S.C.C.; Smits, A.J. Turbulent Pipe Flow at Extreme Reynolds Numbers. *Phys. Rev. Lett.* **2012**, *108*, 094501. [[CrossRef](#)]
29. Ng, H.C.H.; Monty, J.P.; Hutchins, N.; Chong, M.S.; Marusic, I. Comparison of Turbulent Channel and Pipe Flows with Varying Reynolds Number. *Exp. Fluids* **2011**, *51*, 1261–1281. [[CrossRef](#)]
30. Wang, C.Y. On the Low-Reynolds-Number Flow in a Helical Pipe. *J. Fluid Mech.* **1981**, *108*, 185–194. [[CrossRef](#)]
31. Smith, F.T. On the High Reynolds Number Theory of Laminar Flows. *IMA J. Appl. Math.* **1982**, *28*, 207–281. [[CrossRef](#)]

32. Smits, A.J.; McKeon, B.J.; Marusic, I. High-Reynolds Number Wall Turbulence. *Annu. Rev. Fluid Mech.* **2011**, *43*, 353–375. [[CrossRef](#)]
33. Manna, M.; Vacca, A. Scaling Properties of Turbulent Pipe Flow at Low Reynolds Number. *Comput. Fluids* **2001**, *30*, 393–415. [[CrossRef](#)]
34. Dabiri, J.O.; Mohebbi, N.; Fu, M.K. Persistent Laminar Flow at Reynolds Numbers Exceeding 100,000. *arXiv* **2022**, arXiv:2212.02488.
35. Shirbhate, V.S.; Siva Kumar, K.; Madhu Babu, K. Effect of Reynolds Number on Typical Civil Transport Aircraft. *Lecture Notes Mech. Eng.* **2021**, *53*, 471–480. [[CrossRef](#)]
36. Wang, Y.; Liu, D.; Xu, X.; Li, G. Investigation of Reynolds Number Effects on Aerodynamic Characteristics of a Transport Aircraft. *Aerospace* **2021**, *8*, 177. [[CrossRef](#)]
37. Liu, D.; Wang, Y.; Chen, D.; Peng, X.; Xu, X. Numerical Investigation on the Reynolds Number Effects of Supercritical Airfoil. *Procedia Eng.* **2012**, *31*, 103–109. [[CrossRef](#)]
38. Novokhatska, A. Design of an Airfoil by Mathematical Modelling Using Database. *J. Airl. Oper. Aviat. Manag.* **2022**, *1*, 19–26. [[CrossRef](#)]
39. Osusky, M.; Ledezma, G.; Sluyter, G.; Shankaran, S. Reynolds Number Impact on High Pressure Turbine Flows. *Proc. ASME Turbo Expo.* **2023**, *13C*, V13CT32A030. [[CrossRef](#)]
40. Drela, M. Low-Reynolds-Number Airfoil Design for the M.I.T. Daedalus Prototype- A Case Study. *J. Aircr.* **1988**, *25*, 724–732. [[CrossRef](#)]
41. Liu, D.; Xu, X.; Wei, Z.; Dehua, C. Investigation on the Reynolds Number Simulation of Supercritical Airfoil. In Proceedings of the 2013 4th International Conference on Digital Manufacturing and Automation, ICDMA 2013, Shinan, China, 29–30 June 2013; pp. 740–744. [[CrossRef](#)]
42. Gu, Y.; Liu, Y.; Shen, J.; Wang, D. Optimization of Reynolds Number's Effects on Aerodynamic Drag and Automotive Performance. *Theor. Nat. Sci.* **2023**, *13*, 144–149. [[CrossRef](#)]
43. Solmaz, H.; İcingür, Y. Drag Coefficient Determination Of A Bus Model Using Reynolds Number Independence. *Int. J. Automot. Eng. Technol.* **2015**, *4*, 146–151. [[CrossRef](#)]
44. Zhao, G.; Pumera, M. Reynolds Numbers Exhibit Dramatic Influence on Directionality of Movement of Self-Propelled Systems. *Phys. Chem. Chem. Phys.* **2012**, *14*, 6456–6458. [[CrossRef](#)] [[PubMed](#)]
45. Amromin, E.L. Vehicles Drag Reduction with Control of Critical Reynolds Number. *J. Fluids Eng.* **2013**, *135*, 101105. [[CrossRef](#)]
46. Qin, P.; Ricci, A.; Blocken, B. CFD Simulation of Aerodynamic Forces on the DrivAer Car Model: Impact of Computational Parameters. *J. Wind Eng. Ind. Aerodyn.* **2024**, *248*, 105711. [[CrossRef](#)]
47. Haffner, Y.; Li, R.; Meldi, M.; Borée, J. Drag Reduction of a Square-Back Bluff Body under Constant Cross-Wind Conditions Using Asymmetric Shear Layer Forcing. *Int. J. Heat Fluid Flow* **2022**, *96*, 109003. [[CrossRef](#)]
48. Xu, J.; Dong, S.; Maxey, M.R.; Karniadakis, G.E. Turbulent Drag Reduction by Constant Near-Wall Forcing. *J. Fluid Mech.* **2007**, *582*, 79–101. [[CrossRef](#)]
49. Fuaad, P.A.; Baig, M.F.; Khan, B.A. Turbulent Drag Reduction Using Active Control of Buoyancy Forces. *Int. J. Heat Fluid Flow* **2016**, *61*, 585–598. [[CrossRef](#)]
50. Gugulothu, R.; Sanke, N.; Gupta, A.V.S.S.K.S. Numerical Study of Heat Transfer Characteristics in Shell-and-Tube Heat Exchanger. In *Lecture Notes in Mechanical Engineering*; Springer: Singapore, 2019; pp. 375–383. [[CrossRef](#)]
51. Saleem, A.; Kim, M.H. CFD Analysis on the Air-Side Thermal-Hydraulic Performance of Multi-Louvered Fin Heat Exchangers at Low Reynolds Numbers. *Energies* **2017**, *10*, 823. [[CrossRef](#)]
52. Shinde, P.; Lin, C.X. A Heat Transfer and Friction Factor Correlation for Low Air-Side Reynolds Number Applications of Compact Heat Exchangers (1535-RP). *Sci. Technol. Built Environ.* **2017**, *23*, 192–210. [[CrossRef](#)]
53. Al-Amshawee, S.K.A.; Yunus, M.Y.B.M. Electrodialysis Desalination: The Impact of Solution Flowrate (or Reynolds Number) on Fluid Dynamics throughout Membrane Spacers. *Environ. Res.* **2023**, *219*, 115115. [[CrossRef](#)] [[PubMed](#)]
54. Amalia, R.; Safitra, A.G.; Ubudiyah, H. Numerical Study on Heat Transfer and Friction Factor Characteristics of Transition Flow in Shell and Tube Heat Exchanger. In Proceedings of the IES 2019—International Electronics Symposium: The Role of Techno-Intelligence in Creating an Open Energy System Towards Energy Democracy, Surabaya, Indonesia, 27–28 September 2019; pp. 283–286. [[CrossRef](#)]
55. Almurtaji, S.; Ali, N.; Teixeira, J.A.; Addali, A. On the Role of Nanofluids in Thermal-Hydraulic Performance of Heat Exchangers—A Review. *Nanomaterials* **2020**, *10*, 734. [[CrossRef](#)] [[PubMed](#)]
56. Mehta, B.; Subhedar, D.; Panchal, H.; Said, Z. Synthesis, Stability, Thermophysical Properties and Heat Transfer Applications of Nanofluid—A Review. *J. Mol. Liq.* **2022**, *364*, 120034. [[CrossRef](#)]
57. Wang, J.; Yang, X.; Klemeš, J.J.; Tian, K.; Ma, T.; Sunden, B. A Review on Nanofluid Stability: Preparation and Application. *Renew. Sustain. Energy Rev.* **2023**, *188*, 113854. [[CrossRef](#)]
58. Hou, G.; Taherian, H.; Song, Y.; Jiang, W.; Chen, D. A Systematic Review on Optimal Analysis of Horizontal Heat Exchangers in Ground Source Heat Pump Systems. *Renew. Sustain. Energy Rev.* **2022**, *154*, 111830. [[CrossRef](#)]
59. Clifford, M.J.; Cox, S.M.; Finn, M.D. Reynolds Number Effects in a Simple Planetary Mixer. *Chem. Eng. Sci.* **2004**, *59*, 3371–3379. [[CrossRef](#)]
60. Yoon, H.-S.; Chun, H.-H.; Ha, M.-Y. The Study of Flow Structure in a Mixing Tank for Different Reynolds Numbers Using LES. *Trans. Korean Soc. Mech. Eng. B* **2003**, *27*, 1290–1298. [[CrossRef](#)]

61. Mizuno, Y.; Funakoshi, M. Reynolds Number Dependences of Velocity Field and Fluid Mixing in Partitioned-Pipe Mixer. *J. Phys. Soc. Jpn.* **2005**, *74*, 1479–1489. [[CrossRef](#)]
62. Suresh, P.R.; Das, S.K.; Sundararajan, T. Influence of Reynolds Number on the Evolution of a Plane Air Jet Issuing From a Slit. *J. Fluids Eng.* **2007**, *129*, 1288–1296. [[CrossRef](#)]
63. Evrim, C.; Laurien, E. Effect of the Reynolds and Richardson Numbers on Thermal Mixing Characteristics. *Int. J. Heat Mass Transf.* **2021**, *169*, 120917. [[CrossRef](#)]
64. Awad, M.M.; Muzychka, Y.S. Models for Pressure Drop and Heat Transfer in Air Cooled Compact Wavy Fin Heat Exchangers. *J. Enhanc. Heat Transf.* **2011**, *18*, 191–207. [[CrossRef](#)]
65. Sotsu, M. Friction Factor and Reynolds Number Correlation for Finned Tube Bundle of the Air Cooler of Monju Reactor. *Nucl. Eng. Des.* **2022**, *396*, 111893. [[CrossRef](#)]
66. El-Abeedy, E.A.; Busedra, A.A. Effect of Reynolds Number on Inclined Heated Semicircular Ducts at Different Rotations. *Fluid Dyn. Mater. Process.* **2013**, *9*, 153–167. [[CrossRef](#)]
67. Qi, R.; Chen, F.; Xu, L.; Yu, J.; Chen, X. Effects of Reynolds Number on the Overall Characteristics of Flow and Heat Transfer in the Long Micro-Tube with Dimples. *Processes* **2022**, *10*, 2696. [[CrossRef](#)]
68. Mostafapour, K.; Nouri, N.M.; Zeinali, M. The Effects of the Reynolds Number on the Hydrodynamics Characteristics of an AUV. *J. Appl. Fluid Mech.* **2018**, *11*, 343–352. [[CrossRef](#)]
69. Gad-El-Hak, M. Compliant Coatings: A Decade of Progress. *Appl. Mech. Rev.* **1996**, *49*, S147–S157. [[CrossRef](#)]
70. Amini Ferooshani, J.; Sabzpooshani, M. An Approach for the Estimation of Hydrodynamic Coefficients of an Underwater Vehicle in Off-Design Velocities. *J. Mar. Sci. Technol.* **2021**, *26*, 368–381. [[CrossRef](#)]
71. Pan, Y.C.; Zhang, H.X.; Zhou, Q.D. Numerical Prediction of Submarine Hydrodynamic Coefficients Using CFD Simulation. *J. Hydrodyn.* **2012**, *24*, 840–847. [[CrossRef](#)]
72. Zhu, H.; Hu, J.; Alam, M.M.; Ji, C.; Zhou, T. Hydrodynamic Characteristics and Wake Evolution of a Submarine Pipe with the Presence of Gas Leakage at a Low Reynolds Number of 160. *Phys. Fluids* **2022**, *34*, 083609. [[CrossRef](#)]
73. Elahi, S.S.; Lange, E.A.; Lynch, S.P. Effect of Reynolds Number on Turbulent Junction Flow Fluid Dynamics and Heat Transfer. *Int. J. Heat Mass Transf.* **2019**, *142*, 118328. [[CrossRef](#)]
74. Smits, A.J.; Zagarola, M.V. Applications of Dense Gases to Model Testing for Aeronautical and Hydrodynamic Applications. *Meas. Sci. Technol.* **2005**, *16*, 1710. [[CrossRef](#)]
75. Kim, D.; Kim, Y.; Li, J.; Wilson, R.V.; Ezequiel Martin, J.; Carrica, P.M. Boundary Layer Transition Models for Naval Applications: Capabilities and Limitations. *J. Ship Res.* **2019**, *63*, 294–307. [[CrossRef](#)]
76. Liu, J.; Liu, J.; Zhang, Y. Influence of Reynolds Number on the Natural Transition of Boundary Layers over Underwater Axisymmetric Bodies. *Phys. Fluids* **2023**, *35*, 044107. [[CrossRef](#)]
77. He, K.; Pan, Z.; Zhao, W.; Wang, J.; Wan, D. Overview of Research Progress on Numerical Simulation Methods for Turbulent Flows Around Underwater Vehicles. *J. Mar. Sci. Appl.* **2024**, *23*, 1–22. [[CrossRef](#)]
78. Kornev, N.; Shevchuk, I.; Abbas, N.; Anschau, P.; Samarbakhsh, S. Potential and Limitations of Scale Resolved Simulations for Ship Hydrodynamics Applications. *Ship Technol. Res.* **2019**, *66*, 83–96. [[CrossRef](#)]
79. Torobin, L.B.; Gauvin, W.H. Fundamental Aspects of Solids-Gas Flow: Part I: Introductory Concepts and Idealised Sphere Motion in Viscous Regime. *Can. J. Chem. Eng.* **1959**, *37*, 129–141. [[CrossRef](#)]
80. Boger, D.V. Rheology and the Minerals Industry. *Miner. Process. Extr. Metall. Rev.* **2000**, *20*, 1–25. [[CrossRef](#)]
81. Jikazana, A.; Campo, P.; McAdam, E.J. Hydrodynamics (Reynolds Number) Determine Scaling, Nucleation and Crystal Growth Kinetics in Membrane Distillation Crystallisation. *J. Memb. Sci.* **2023**, *685*, 121909. [[CrossRef](#)]
82. Edwards, D.A.; Shapiro, M.; Bar-Yoseph, P.; Shapira, M. The Influence of Reynolds Number upon the Apparent Permeability of Spatially Periodic Arrays of Cylinders. *Phys. Fluids A Fluid. Dyn.* **1990**, *2*, 45–55. [[CrossRef](#)]
83. Wrench, D.; Parashar, T.N.; Oughton, S.; de Lange, K.; Frea, M. What Is the Reynolds Number of the Solar Wind? *Astrophys. J.* **2024**, *961*, 182. [[CrossRef](#)]
84. Ryan, N.W.; Johnson, M.M. Transition from Laminar to Turbulent Flow in Pipes. *AIChE J.* **1959**, *5*, 433–435. [[CrossRef](#)]
85. Bankston, C.A. The Transition from Turbulent to Laminar Gas Flow in a Heated Pipe. *J. Heat Transf.* **1970**, *92*, 569–579. [[CrossRef](#)]
86. Spriggs, H.D. Comments on Transition from Laminar to Turbulent Flow. *Ind. Eng. Chem. Fundam.* **1973**, *12*, 286–290. [[CrossRef](#)]
87. Barr, D. The Transition from Laminar to Turbulent Flow. *Proc. Inst. Civ. Eng.* **1980**, *69*, 555–562. [[CrossRef](#)]
88. Happel, J.; Brenner, H. *Low Reynolds Number Hydrodynamics; Mechanics of Fluids and Transport Processes*; Springer: Dordrecht, The Netherlands, 1983; Volume 1, ISBN 978-90-247-2877-0.
89. Hinch, E.J. Hydrodynamics at Low Reynolds Numbers: A Brief and Elementary Introduction. In *Disorder and Mixing*; NATO ASI Series; Springer: Dordrecht, The Netherlands, 1988; Volume 152, pp. 43–56. [[CrossRef](#)]
90. Khayat, R.E.; Eu, B.C. Generalized Hydrodynamics and Reynolds-Number Dependence of Steady-Flow Properties in the Cylindrical Couette Flow of Lennard-Jones Fluids. *Phys. Rev. A* **1989**, *40*, 946. [[CrossRef](#)]
91. Szwalek, J.L.; Larsen, C.M. Reynolds Number Effects on Hydrodynamic Coefficients for Pure In-Line and Pure Cross-Flow Forced Vortex Induced Vibrations. In Proceedings of the International Conference on Offshore Mechanics and Arctic Engineering—OMAE, Honolulu, HI, USA, 31 May–5 June 2009; Volume 5, pp. 439–452. [[CrossRef](#)]
92. Dewsbury, K.H.; Karamanev, D.G.; Margaritis, A. Rising Solid Sphere Hydrodynamics at High Reynolds Numbers in Non-Newtonian Fluids. *Chem. Eng. J.* **2002**, *87*, 129–133. [[CrossRef](#)]

93. Meister, M.; Burger, G.; Rauch, W. On the Reynolds Number Sensitivity of Smoothed Particle Hydrodynamics. *J. Hydraul. Res.* **2014**, *52*, 824–835. [[CrossRef](#)]
94. Enayet, M.M.; Gibson, M.M.; Taylor, A.M.K.P.; Yianneskis, M. Laser-Doppler Measurements of Laminar and Turbulent Flow in a Pipe Bend. *Int. J. Heat Fluid Flow* **1982**, *3*, 213–219. [[CrossRef](#)]
95. Xiao, Z.; Guo, L.; Feng, D.; Lai, S.; Hu, Z. Numerical Study on the Scale Effects of the Ship Resistance and Form Factor. In Proceedings of the 2018 IEEE 8th International Conference on Underwater System Technology: Theory and Application (USYS 2018), Wuhan, China, 1–3 December 2018. [[CrossRef](#)]
96. Matsuda, S.; Katsui, T. Hydrodynamic Forces and Wake Distribution of Various Ship Shapes Calculated Using a Reynolds Stress Model. *J. Mar. Sci. Eng.* **2022**, *10*, 777. [[CrossRef](#)]
97. Parolini, N. Computational Fluid Dynamics for Naval Engineering Problems. Ph.D. Thesis, École Polytechnique Fédérale de Lausanne, Lausanne, Switzerland, 2004.
98. Eça, L.; Kerkvliet, M.; Toxopeus, S.L. Using Validation Metrics to Assess RANS Turbulence Models Performance at Full Scale Reynolds Numbers. In Proceedings of the ASME International Mechanical Engineering Congress and Exposition, Proceedings (IMECE), New Orleans, LA, USA, 29 October–2 November 2023; Volume 9, p. 13. [[CrossRef](#)]
99. Speziale, C. A Review of Reynolds Stress Models for Turbulent Shear Flows. In *Final Report Institute for Computer Applications in Science and Engineering*; NTRS—NASA Technical Reports Server: Hampton, Virginia, USA, 1995.
100. Valentine, D. *Reynolds-Averaged Navier-Stokes Codes and Marine Propulsor Analysis*; Naval Surface Warfare Center: Bethesda, MD, USA, 1993.
101. Gross, A.; Kremheller, A.; Fasel, H. Simulation of Flow over Suboff Bare Hull Model. In Proceedings of the 49th AIAA Aerospace Sciences Meeting including the New Horizons Forum and Aerospace Exposition, Orlando, FL, USA, 4–7 January 2011; American Institute of Aeronautics and Astronautics: Reston, VA, USA, 2011.
102. Sener, M.Z.; Aksu, E. The Numerical Investigation of the Rotation Speed and Reynolds Number Variations of a NACA 0012 Airfoil. *Ocean Eng.* **2022**, *249*, 110899. [[CrossRef](#)]
103. Ferreira, J.W.; Vanessa, L.; Da, M.; Judice, R.; Lucas Heldt, L. Resistências Hidrodinâmicas Observados Em Projetos Navais. *Rev. Ciênc. Exatas E Tecnol.* **2021**, *16*, 2–6. [[CrossRef](#)]
104. Tatsuo Nishikawa, by; Yoshinobu Yamade, M.; Masaru Sakuma, N.; Chisachi Kato, N. Application of Fully-Resolved Large Eddy Simulation to KVLCC2-Bare Hull Double Model at Model Ship Reynolds Number. *J. Jpn. Soc. Nav. Archit. Ocean. Eng.* **2012**, *16*, 1–9. [[CrossRef](#)]
105. Zhang, Z.; Liu, H.; Zhu, S.; Zhao, F. Application of CFD in Ship Engineering Design Practice and Ship Hydrodynamics. *J. Hydrodyn. B* **2006**, *18*, 315–322. [[CrossRef](#)]
106. Lissaman, P.B.S. Low-Reynolds-Number Airfoils. *Annu. Rev. Fluid Mech.* **1983**, *15*, 223–239. [[CrossRef](#)]
107. Mueller, T.J.; DeLaurier, J.D. Aerodynamics of Small Vehicles. *Annu. Rev. Fluid Mech.* **2003**, *35*, 89–111. [[CrossRef](#)]
108. Hemanth, V.; Kushal, K.S.; Varun, S.S. Aerodynamic Study on Low Reynolds Number Aerofoil. *ACS J. Sci. Eng.* **2024**, *4*, 39–57. [[CrossRef](#)]
109. Heine, B.; Mack, S.; Kurz, A.; Gross, A.; Fasel, H. Aerodynamic Scaling of General Aviation Airfoil for Low Reynolds Number Application. In Proceedings of the 38th Fluid Dynamics Conference and Exhibit, Seattle, WA, USA, 23–26 June 2008; American Institute of Aeronautics and Astronautics: Reston, VA, USA, 2008; pp. 2008–4410.
110. Hu, H.; Yang, Z.; Igarashi, H. Aerodynamic Hysteresis of a Low-Reynolds-Number Airfoil. *J. Aircr.* **2007**, *44*, 2083–2086. [[CrossRef](#)]
111. Spreitr, J.; Steffen, P. *Effect of Mach and Reynolds Numbers on Maximum Lift Coefficient*; NTRS—NASA Technical Reports Server: Hampton, VA, USA, 1946.
112. Selig, M.S.; Maughmer, M.D.; Somers, D.M. Natural-Laminar-Flow Airfoil for General-Aviation Applications. *J. Aircr.* **1995**, *32*, 710–715. [[CrossRef](#)]
113. Dryden, H.L. Turbulence, Companion of Reynolds Number. *J. Aeronaut. Sci.* **1934**, *1*, 67–75. [[CrossRef](#)]
114. Edwini-Bonsu, S.; Steffler, P.M. Dynamics of Air Flow in Sewer Conduit Headspace. *J. Hydraul. Eng.* **2006**, *132*, 791–799. [[CrossRef](#)]
115. Edwini-Bonsu, S.; Steffler, P.M. Air Flow in Sanitary Sewer Conduits Due to Wastewater Drag: A Computational Fluid Dynamics Approach. *J. Environ. Eng. Sci.* **2004**, *3*, 331–342. [[CrossRef](#)]
116. Li, Z.; Wang, B.; Wang, F.; Sun, B.; Li, L. Flow Dynamics and Turbulent Coherent Structures around Sediment Reduction Plates of a Sewer System. *J. Environ. Manag.* **2024**, *366*, 121594. [[CrossRef](#)] [[PubMed](#)]
117. da Silva, A.M.A.; Bolisetti, T. A Method for the Formulation of Reynolds Number Functions. *Can. J. Civ. Eng.* **2000**, *27*, 829–833. [[CrossRef](#)]
118. Cahyanto, A.D.; Ilman, I.N.; Putra, A. Penentuan Bilangan Reynold Dan Froude, Redesign Zona Sedimentasi Rectangular Dengan Plate Settler Dan Tube Settler, Water Treatment Plant (Wtp), Kawasan Industri Dan Perumahan “X”, Kabupaten Bekasi. *J. Poli-Tekno.* **2023**, *22*, 71–83. [[CrossRef](#)]
119. Halliwell, A.R.; Barr, D.I.H.; Saul, A.J.; Burrows, R.; Oakley, H.R.; Ali, K.H.M. Discussion. The Use of Hydraulic Models to Examine the Performance of Storm-Sewage Overflows. *Proc. Inst. Civ. Eng.* **1981**, *71*, 277–282. [[CrossRef](#)]
120. Soares-Frazão, S. Wastewater Hydraulics. *J. Hydraul. Res.* **2011**, *49*, 842–843. [[CrossRef](#)]
121. Altowayti, W.A.H.; Othman, N.; Tajarudin, H.A.; Al-Dhaqm, A.; Asharuddin, S.M.; Al-Gheethi, A.; Alsharif, A.F.; Salem, A.A.; Md Din, M.F.; Fitriani, N.; et al. Evaluating the Pressure and Loss Behavior in Water Pipes Using Smart Mathematical Modelling. *Water* **2021**, *13*, 3500. [[CrossRef](#)]

122. Carvajal, J.; Zambrano, W.; Gómez, N.; Saldarriaga, J. Turbulent Flow in PVC Pipes in Water Distribution Systems. *Urban Water J.* **2020**, *17*, 503–511. [[CrossRef](#)]
123. Liou, C.P. Limitations and Proper Use of the Hazen-Williams Equation. *J. Hydraul. Eng.* **1998**, *124*, 951–954. [[CrossRef](#)]
124. Buchberger, S.G.; Wu, L. Model for Instantaneous Residential Water Demands. *J. Hydraul. Eng.* **1995**, *121*, 232–246. [[CrossRef](#)]
125. Kaltenbacher, S.; Steinberger, M.; Horn, M. Applied Pipe Roughness Identification of Water Networks: Consideration of All Flow Regimes. *IEEE Trans. Control Syst. Technol.* **2023**, *31*, 676–691. [[CrossRef](#)]
126. Montalvo, I.; Izquierdo, J.; Pérez, R.; Tung, M.M. Particle Swarm Optimization Applied to the Design of Water Supply Systems. *Comput. Math. Appl.* **2008**, *56*, 769–776. [[CrossRef](#)]
127. Yazdani, A.; Jeffrey, P. Complex Network Analysis of Water Distribution Systems. *Chaos* **2011**, *21*, 016111. [[CrossRef](#)] [[PubMed](#)]
128. Sigg, K.C.; Coffield, R.D. Qualification of a Method to Calculate the Irrecoverable Pressure Loss in High Reynolds Number Piping Systems. In Proceedings of the ASME/JSME Joint Fluids Engineering Conference, Honolulu, HI, USA, 6–10 July 2003; Volume 36975, pp. 143–151. [[CrossRef](#)]
129. Koch, P. The Influence of Reynolds Number and Size Effects on Pressure Loss Factors of Ductwork Components. *Build. Serv. Eng. Res. Technol.* **2006**, *27*, 261–283. [[CrossRef](#)]
130. Savić, V.; Knežević, D.; Lovrec, D.; Jocanović, M.; Karanović, V. Determination of Pressure Losses in Hydraulic Pipeline Systems by Considering Temperature and Pressure. *J. Mech. Eng.* **2009**, *55*, 237–443.
131. Tawackolian, K.; Kriegel, M. Turbulence Model Performance for Ventilation Components Pressure Losses. *Build. Simul.* **2022**, *15*, 389–399. [[CrossRef](#)]
132. Dosunmu, I.T.; Shah, S.N. Pressure Drop Predictions for Laminar Pipe Flow of Carreau and Modified Power Law Fluids. *Can. J. Chem. Eng.* **2015**, *93*, 929–934. [[CrossRef](#)]
133. Dutta, P.; Nandi, N. Study on Pressure Drop Characteristics of Single Phase Turbulent Flow in Pipe Bend for High Reynolds Number. *ARPJ. Eng. Appl. Sci.* **2015**, *10*, 2221–2226.
134. El-Adawy, M.; Farid, A.H.; Hassan, M.A.; Abady, M.; Medhat, D.; Abdullatif, H.; Hassan, O.; Thabet, S.M. Low Reynolds Number Wing Design for Unmanned Aerial Vehicle: A Case Study. *Am. J. Eng. Appl. Sci.* **2022**, *15*, 264–273. [[CrossRef](#)]
135. Campbell, R.L.; Carter, M.B.; Pendergraft, O.C.; Friedman, D.M.; Serrano, L. Design and Testing of a Blended Wing Body with Boundary Layer Ingestion Nacelles at High Reynolds Numbers (Invited). In Proceedings of the 43rd AIAA Aerospace Sciences Meeting and Exhibit—Meeting Papers, Reno, NV, USA, 10–13 January 2005; pp. 7145–7171. [[CrossRef](#)]
136. Lin, P.; Wu, J.; Lu, L.; Xiong, N.; Liu, D.; Su, J.; Liu, G.; Tao, Y.; Wu, J.; Liu, X. Investigation on the Reynolds Number Effect of a Flying Wing Model with Large Sweep Angle and Small Aspect Ratio. *Aerospace* **2022**, *9*, 523. [[CrossRef](#)]
137. Kegerise, M.A.; Neuhart, D.H.; Hannon, J.A.; Rumsey, C.L. An Experimental Investigation of a Wing-Fuselage Junction Model in the Nasa Langley 14-by 22-Foot Subsonic Wind Tunnel. In Proceedings of the AIAA Scitech 2019 Forum, San Diego, CA, USA, 7–11 January 2019. [[CrossRef](#)]
138. Gatard, J.; Costes, M.; Kroll, N.; Renzoni, P.; Kokkalis, A.; Rocchetto, A.; Serr, C.; Larrey, E.; Filippone, A.; Wehr, D. High Reynolds Number Helicopter Fuselage Test in the ONERA F1 Pressurised Wind Tunnel. In *Proceedings of the Rotorcraft Forum*; Institute of Aerodynamics and Fluid Dynamics: Dresden, Germany, 1997.
139. Polharnus, E.C. *A Review of Some Reynolds Number Effects Related to Bodies at High Angles of Attack*; Newport News; NASA: Hampton, VA, USA, 1984.
140. Roberts, L.S.; Finnis, M.V.; Knowles, K. Characteristics of Boundary-Layer Transition and Reynolds-Number Sensitivity of Three-Dimensional Wings of Varying Complexity Operating in Ground Effect. *J. Fluids Eng.* **2016**, *138*, 091106. [[CrossRef](#)]
141. Mokhtar, W.A. A Numerical Study of High-Lift Single Element Airfoils with Ground Effect for Racing Cars. *SAE Int.* **2005**, *114*, 682–688. [[CrossRef](#)]
142. Hoque, M.A.; Rahman, M.S.; Rimi, K.N.; Alif, A.R.; Haque, M.R. Enhancing Formula Student Car Performance: Nose Shape Optimization via Adjoint Method. *Results Eng.* **2023**, *20*, 101636. [[CrossRef](#)]
143. Lei, J.; He, J. Adjoint-Based Aerodynamic Shape Optimization for Low Reynolds Number Airfoils. *J. Fluids Eng. Trans. ASME* **2016**, *138*, 021401. [[CrossRef](#)]
144. Eftekhari, H.; Al-Obaidi, A.S.M.; Eftekhari, S. The Effect of Spoiler Shape and Setting Angle on Racing Cars Aerodynamic Performance. *Indones. J. Sci. Technol.* **2020**, *5*, 11–20. [[CrossRef](#)]
145. Ravi, S. The Influence of Turbulence on a Flat Plate Aerofoil at Reynolds Numbers Relevant to MAVs. Ph.D. Thesis, RMIT University, Melbourne, VIC, Australia, 2011.
146. Genç, M.S.; Karasu, İ.; Açikel, H.H.; Akpolat, M.T.; Genç, M.S.; Karasu, İ.; Açikel, H.H.; Akpolat, M.T. Low Reynolds Number Flows and Transition. In *Low Reynolds Number Aerodynamics and Transition*; IntechOpen: London, UK, 2012. [[CrossRef](#)]
147. Shukla, D.; Komerath, N. Multicopter Drone Aerodynamic Interaction Investigation. *Drones* **2018**, *2*, 43. [[CrossRef](#)]
148. Pérez Gordillo, A.M.; Escobar, J.A.; Lopez Mejia, O.D. Influence of the Reynolds Number on the Aerodynamic Performance of a Small Rotor. *Aerospace* **2023**, *10*, 130. [[CrossRef](#)]
149. Liu, H.; Ravi, S.; Kolomenskiy, D.; Tanaka, H. Biomechanics and Biomimetics in Insect-Inspired Flight Systems. *Philos. Trans. R. Soc. B Biol. Sci.* **2016**, *371*, 20150390. [[CrossRef](#)]
150. Li, F.; Bai, P.; Shi, W.; Li, J.W. Low Reynolds Number Aerodynamics of Micro Air Vehicles. *Adv. Mech.* **2007**, *37*, 257–268. [[CrossRef](#)]

151. le Balleur, J.C.; Peyret, R.; Viviand, H. Numerical Studies in High Reynolds Number Aerodynamics. *Comput. Fluids* **1980**, *8*, 1–30. [[CrossRef](#)]
152. Owens, L.R.; Wahls, R.A.; Elzey, M.B.; Hamner, M.P. Reynolds Number Effects on Off-Design Stability and Control Characteristics of Supersonic Transports. *J. Aircr.* **2007**, *44*, 134–143. [[CrossRef](#)]
153. Wahls, R.A.; Owens, L.R.; Rivers, S.M.B. Reynolds Number Effects on a Supersonic Transport at Transonic Conditions. In Proceedings of the 39th AIAA Aerospace Sciences Meeting & Exhibit, Reno, NV, USA, 8–11 January 2001. [[CrossRef](#)]
154. Owens, L.; Wahls, R. Reynolds Number Effects on a Supersonic Transport at Subsonic High-Lift Conditions. In Proceedings of the 39th AIAA Aerospace Sciences Meeting & Exhibit, Reno, NV, USA, 8–11 January 2001. [[CrossRef](#)]
155. Owens, L.R.; Wahls, R.A.; Elzey, M.B.; Hamner, M.P. Reynolds Number Effects on the Stability & Control Characteristics of a Supersonic Transport. In Proceedings of the 40th AIAA Aerospace Sciences Meeting and Exhibit, Reno, NV, USA, 14–17 January 2002. [[CrossRef](#)]
156. Johnson, J.A.; Zhang, Y.; Johnson, L.E. Evidence of Reynolds Number Sensitivity in Supersonic Turbulent Shocklets. *AIAA J.* **1988**, *26*, 502–504. [[CrossRef](#)]
157. Kawaji, M.; Kawahara, A.; Chung, P.M.Y. Instantaneous Velocity Profiles and Characteristics of Pressure-Driven Flow in Microchannels. In Proceedings of the ASME 2001 International Mechanical Engineering Congress and Exposition, New York, NY, USA, 11–16 November 2001; pp. 131–141. [[CrossRef](#)]
158. Liu, D.; Garimella, S.V. Investigation of Liquid Flow in Microchannels. *J. Thermophys. Heat Trans.* **2004**, *18*, 65–72. [[CrossRef](#)]
159. Yao, J.; Yao, Y.F.; Patel, M.K.; Mason, P.J. On Reynolds Number and Scaling Effects in Microchannel Flows. *Eur. Phys. J. Appl. Phys.* **2007**, *37*, 229–235. [[CrossRef](#)]
160. Peng, X.F.; Peterson, G.P.; Wang, B.X. Frictional Flow Characteristics of Water Flowing through Rectangular Microchannels. *Exp. Heat Transf.* **1994**, *7*, 249–264. [[CrossRef](#)]
161. Pfund, D.; Rector, D.; Shekarriz, A.; Popescu, A.; Welty, J. Pressure Drop Measurements in a Microchannel. *AIChE J.* **2000**, *46*, 1496–1507. [[CrossRef](#)]
162. Koo, J.; Kleinstreuer, C. Liquid Flow in Microchannels: Experimental Observations and Computational Analyses of Microfluidics Effects. *J. Micromech. Microeng.* **2003**, *13*, 568. [[CrossRef](#)]
163. Tao, R.; Jin, Y.; Gao, X.; Li, Z. Flow Characterization in Converging-Diverging Microchannels. *Phys. Fluids* **2018**, *30*, 112004. [[CrossRef](#)]
164. Chaudhari, P.; Kapoor, A.; Awasthi, Y.; Thakur, A.K.; Kumar, R. Numerical Simulation of Fluid Flow in Microchannels with Induced Irregularities. *Int. J. Chem. React. Eng.* **2023**, *21*, 1443–1452. [[CrossRef](#)]
165. Wang, G.R.; Yang, F.; Zhao, W. There Can Be Turbulence in Microfluidics at Low Reynolds Number. *Lab Chip* **2014**, *14*, 1452–1458. [[CrossRef](#)] [[PubMed](#)]
166. Wang, G.; Yang, F.; Zhao, W.; Chen, C.P. On Micro-Electrokinetic Scalar Turbulence in Microfluidics at a Low Reynolds Number. *Lab Chip* **2016**, *16*, 1030–1038. [[CrossRef](#)] [[PubMed](#)]
167. Rasouli, M.R.; Abouei Mehrizi, A.; Lashkaripour, A. Numerical Study on Low Reynolds Mixing of T-Shaped Micro-Mixers with Obstacles. *Chall. Nano Micro Scale Sci. Technol.* **2015**, *3*, 68–76. [[CrossRef](#)]
168. Shanko, E.S.; van de Burgt, Y.; Anderson, P.D.; den Toonder, J.M.J. Microfluidic Magnetic Mixing at Low Reynolds Numbers and in Stagnant Fluids. *Micromachines* **2019**, *10*, 731. [[CrossRef](#)] [[PubMed](#)]
169. Paya, N.; Dankovic, T.; Feinerman, A. A Microfluidic Mixer Fabricated From Compliant Thermoplastic Films. *J. Undergrad. Res. Univ. Ill. Chic.* **2008**, *2*. [[CrossRef](#)]
170. Sochol, R.D.; Lu, A.; Lei, J.; Iwai, K.; Lee, L.P.; Lin, L. Microfluidic Bead-Based Diodes with Targeted Circular Microchannels for Low Reynolds Number Applications. *Lab. Chip* **2014**, *14*, 1585–1594. [[CrossRef](#)]
171. Sochol, R.D.; Glick, C.C.; Lee, K.Y.; Brubaker, T.; Lu, A.; Wah, M.; Gao, S.; Hicks, E.; Wolf, K.T.; Iwai, K.; et al. Single-Layer “Domino” Diodes via Optofluidic Lithography for Ultra-Low Reynolds Number Applications. In Proceedings of the IEEE International Conference on Micro Electro Mechanical Systems (MEMS), Taipei, Taiwan, 20–24 January 2013; pp. 153–156. [[CrossRef](#)]
172. Abdul Hamid, I.S.L. Reynolds Number Effects in Designing a Micromixer for Biomems Application. Master’s Thesis, Universiti Tun Hussein Onn, Johor, Malaysia, 2008.
173. Yan, S.R.; Sedeh, S.N.; Toghraie, D.; Afrand, M.; Foong, L.K. Analysis and Manegement of Laminar Blood Flow inside a Cerebral Blood Vessel Using a Finite Volume Software Program for Biomedical Engineering. *Comput. Methods Programs Biomed.* **2020**, *190*, 105384. [[CrossRef](#)] [[PubMed](#)]
174. Cape, E.G.; Jones, M.; Yamada, I.; VanAuker, M.D.; Valdes-Cruz, L.M. Turbulent/Viscous Interactions Control Doppler/Catheter Pressure Discrepancies in Aortic Stenosis: The Role of the Reynolds Number. *Circulation* **1996**, *94*, 2975–2981. [[CrossRef](#)]
175. Adams, J.C.; Jiamsripong, P.; Belohlavek, M.; McMahon, E.M.; Marupakula, V.; Heys, J.; Chaliki, H.P. Potential Role of Reynolds Number in Resolving Doppler- and Catheter-Based Transvalvular Gradient Discrepancies in Aortic Stenosis. *J. Heart Valve Dis.* **2011**, *20*, 159–164. [[PubMed](#)]
176. Day, S.W.; Lemire, P.P.; Flack, R.D.; McDaniel, J.C. Effect of Reynolds Number on Performance of a Small Centrifugal Pump. In Proceedings of the ASME/JSME Joint Fluids Engineering Conference, Honolulu, HI, USA, 6–10 July 2003; pp. 1893–1899. [[CrossRef](#)]

177. Magin, C.M.; Long, C.J.; Cooper, S.P.; Ista, L.K.; López, G.P.; Brennan, A.B. Engineered Antifouling Microtopographies: The Role of Reynolds Number in a Model That Predicts Attachment of Zoospores of *Ulva* and Cells of *Cobetia Marina*. *Biofouling* **2010**, *26*, 719–727. [[CrossRef](#)]
178. Javadzadegan, A.; Shimizu, Y.; Behnia, M.; Ohta, M. Correlation between Reynolds Number and Eccentricity Effect in Stenosed Artery Models. *Technol. Health Care* **2013**, *21*, 357–367. [[CrossRef](#)]
179. Asgharzadeh, H.; Borazjani, I. Effects of Reynolds and Womersley Numbers on the Hemodynamics of Intracranial Aneurysms. *Comput. Math. Methods Med.* **2016**, *2016*, 7412926. [[CrossRef](#)] [[PubMed](#)]
180. Shinbrot, T. *Biomedical Fluid Dynamics*; Oxford University Press: Oxford, UK, 2019; ISBN 9780198812586.
181. Nachtigall, W. Some Aspects of Reynolds Number Effects in Animals. *Math. Methods Appl. Sci.* **2001**, *24*, 1401–1408. [[CrossRef](#)]
182. Golestanian, R.; Yeomans, J.M.; Uchida, N. Hydrodynamic Synchronization at Low Reynolds Number. *Soft Matter* **2011**, *7*, 3074–3082. [[CrossRef](#)]
183. Winkler, R.G. Low Reynolds Number Hydrodynamics and Mesoscale Simulations. *Eur. Phys. J. Spec. Top.* **2016**, *225*, 2079–2097. [[CrossRef](#)]
184. Leoni, M.; Liverpool, T.B. Hydrodynamic Synchronization of Nonlinear Oscillators at Low Reynolds Number. *Phys. Rev. E Stat. Nonlin Soft Matter Phys.* **2012**, *85*, 040901. [[CrossRef](#)]
185. Acharya, S.; Nayak, B.; Mishra, S.R. Illustration of the Reynolds Number on Micropolar Nanofluid Flow through a Permeable Medium Due to the Interaction of Thermal Radiation. *Waves Random Complex. Media* **2022**, 1–18. [[CrossRef](#)]
186. Mi, X.B.; Chwang, A.T. Molecular Dynamics Simulations of Nanochannel Flows at Low Reynolds Numbers. *Molecules* **2003**, *8*, 193–206. [[CrossRef](#)]
187. Jaeger, R.; Ren, J.; Xie, Y.; Sundararajan, S.; Olsen, M.G.; Ganapathysubramanian, B. Nanoscale Surface Roughness Affects Low Reynolds Number Flow: Experiments and Modeling. *Appl. Phys. Lett.* **2012**, *101*, 184102. [[CrossRef](#)]
188. Fan, D.L.; Zhu, F.Q.; Cammarata, R.C.; Chien, C.L. Manipulation of Nanowires in Suspension by Ac Electric Fields. *Appl. Phys. Lett.* **2004**, *85*, 4175–4177. [[CrossRef](#)]
189. Jeon, S.; Malyarchuk, V.; White, J.O.; Rogere, J.A. Optically Fabricated Three Dimensional Nanofluidic Mixers for Microfluidic Devices. *Nano Lett.* **2005**, *5*, 1351–1356. [[CrossRef](#)] [[PubMed](#)]
190. Ghosh, A.; Mandal, P.; Karmakar, S.; Ghosh, A. Analytical Theory and Stability Analysis of an Elongated Nanoscale Object under External Torque. *Phys. Chem. Chem. Phys.* **2013**, *15*, 10817–10823. [[CrossRef](#)] [[PubMed](#)]
191. Koplik, J.; Banavar, J.R. Physics of Fluids at Low Reynolds Numbers—A Molecular Approach. *Comput. Phys.* **1998**, *12*, 424–431. [[CrossRef](#)]
192. Cavalcanti, A.; Hogg, T.; Shirinzadeh, B. Nanorobotics System Simulation in 3D Workspaces with Low Reynolds Number. In Proceedings of the 2006 IEEE International Symposium on Micro-Nano Mechanical and Human Science, MHS, Nagoya, Japan, 5–8 November 2006. [[CrossRef](#)]
193. Davis, H.; Kottas, H.; Moody, A.M.G. The Influence of Reynolds Number on the Performance of Turbomachinery. *J. Fluids Eng.* **1951**, *73*, 499–503. [[CrossRef](#)]
194. Strub, A.R.; Bonciani, L.; Borer, C.J.; Casey, M.V.; Cole, S.L.; Cook, B.B.; Kotzur, J.; Simon, H.; Strite, M.A. Influence of the Reynolds Number on the Performance of Centrifugal Compressors. *J. Turbomach.* **1987**, *109*, 541–544. [[CrossRef](#)]
195. Wiesner, F.J. A New Appraisal of Reynolds Number Effects on Centrifugal Compressor Performance. *J. Eng. Power* **1979**, *101*, 384–392. [[CrossRef](#)]
196. Quin, D.; Grimes, R. The Effect of Reynolds Number on Microaxial Flow Fan Performance. *J. Fluids Eng.* **2008**, *130*, 1011011. [[CrossRef](#)]
197. Carpenter, C. Reynolds Number Is Important in Understanding Wax Deposition. *J. Pet. Technol.* **2018**, *70*, 94–95. [[CrossRef](#)]
198. Hirsch, C.; Tartinville, B. Reynolds-Averaged Navier-Stokes Modelling for Industrial Applications and Some Challenging Issues. *Int. J. Comput. Fluid Dyn.* **2009**, *23*, 295–303. [[CrossRef](#)]
199. Jeong, G.S.; Chung, S.; Kim, C.B.; Lee, S.H. Applications of Micromixing Technology. *Analyst* **2010**, *135*, 460–473. [[CrossRef](#)] [[PubMed](#)]
200. Heinz, S.; Roekaerts, D. Modelling of Turbulent Reacting Flows: Reynolds and Damkoehler Number Effects. In Proceedings of the First Symposium on Turbulence and Shear Flow Phenomena, Santa Barbara, CA, USA, 12–15 September 1999; Begel House Inc.: Santa Barbara, CA, USA, 1999; pp. 339–344. [[CrossRef](#)]
201. Heidarinejad, G.; Ghoniem, A. Vortex Simulation of the Reacting Shear Layer—Effects of Reynolds and Damkohler Numbers. In Proceedings of the 27th Aerospace Sciences Meeting, Reno, NV, USA, 9–12 January 1989. [[CrossRef](#)]
202. Patterson, G.K. Application of Turbulence Fundamentals to Reactor Modelling and Scaleup. *Chem. Eng. Commun.* **1981**, *8*, 25–52. [[CrossRef](#)]
203. Gladden, L.F.; Sederman, A.J. Magnetic Resonance Imaging and Velocity Mapping in Chemical Engineering Applications. *Annu. Rev. Chem. Biomol. Eng.* **2017**, *8*, 227–247. [[CrossRef](#)] [[PubMed](#)]
204. Mishra, P.; Ein-Mozaffari, F. Using Statistical and Experimental Methods to Investigate the Mixing of Dense Slurries with Coaxial Mixers: Effects of Design Parameters and Novel Equations for Power and Reynolds Numbers. *Ind. Eng. Chem. Res.* **2021**, *60*, 6306–6326. [[CrossRef](#)]
205. Zhou, Z.; Rujin, M. Numerical Simulation Study of the Reynolds Number Effect on Two Bridge Decks Based on the Deterministic Vortex Method. *Wind Struct.* **2010**, *13*, 347–362. [[CrossRef](#)]

206. Liu, Q.; Ma, W.; Liu, X. Reynolds Number Effect on Bridge Wind Engineering. *Wind Eng. JAWWE* **2014**, *39*, 340–343. [[CrossRef](#)]
207. Matsuda, K.; Cooper, K.R.; Tanaka, H.; Tokushige, M.; Iwasaki, T. An Investigation of Reynolds Number Effects on the Steady and Unsteady Aerodynamic Forces on a 1:10 Scale Bridge Deck Section Model. *J. Wind Eng. Ind. Aerodyn.* **2001**, *89*, 619–632. [[CrossRef](#)]
208. Schewe, G.; Larsen, A. Reynolds Number Effects in the Flow around a Bluff Bridge Deck Cross Section. *J. Wind Eng. Ind. Aerodyn.* **1998**, *74–76*, 829–838. [[CrossRef](#)]
209. Lee, S.; Kwon, S.D.; Yoon, J. Reynolds Number Sensitivity to Aerodynamic Forces of Twin Box Bridge Girder. *J. Wind Eng. Ind. Aerodyn.* **2014**, *127*, 59–68. [[CrossRef](#)]
210. Schewe, G. Influence of the Reynolds-Number on Flow Induced Vibrations of Generic Bridge Sections. In Proceedings of the International Conference on Bridges, Dubrovnik, Croatia, 21–24 May 2006; SECON HDGK: Göttingen, Germany, 2006; pp. 351–358.
211. Kazutoshi, M.; Masafumi, T.; Tooru, I. Reynolds Number Effects on the Steady and Unsteady Aerodynamic Forces Acting on the Bridge Deck Sections of Long-Span Suspension Bridge. *IHI Eng. Rev.* **2007**, *40*, 12–26.
212. Hui, M.C.H.; Zhou, Z.Y.; Chen, A.R.; Xiang, H.F. The Effect of Reynolds Numbers on the Steady State Aerodynamic Force Coefficients of the Stonecutters Bridge Deck Section. *Wind Struct.* **2008**, *11*, 179–192. [[CrossRef](#)]
213. Kargarmoakhar, R.; Chowdhury, A.G.; Irwin, P.A. Reynolds Number Effects on Twin Box Girder Long Span Bridge Aerodynamics. *Wind Struct.* **2015**, *20*, 327–347. [[CrossRef](#)]
214. Zwicky, F. Reynolds' Numbers for Extragalactic Nebulae. *Astrophys. J.* **1941**, *93*, 411. [[CrossRef](#)]
215. Canuto, V.M.; Christensen-Dalsgaard, J. Turbulence in Astrophysics: Stars<sup>1</sup>. *Annu. Rev. Fluid Mech.* **1998**, *30*, 167–198. [[CrossRef](#)]
216. Lazarian, A.; Kowal, G.; Takamoto, M.; de Gouveia Dal Pino, E.M.; Cho, J. Theory and Applications of Non-Relativistic and Relativistic Turbulent Reconnection. *Magn. Reconnect. Concepts Appl.* **2016**, *427*, 409–471. [[CrossRef](#)]
217. Mason, J.; Perez, J.C.; Cattaneo, F.; Boldyrev, S. Extended Scaling Laws in Numerical Simulations of Magnetohydrodynamic Turbulence. *Astrophys. J. Lett.* **2011**, *735*, L26. [[CrossRef](#)]
218. Zhou, Y. Unification and Extension of the Similarity Scaling Criteria and Mixing Transition for Studying Astrophysics Using High Energy Density Laboratory Experiments or Numerical Simulations. *Phys. Plasmas* **2007**, *14*, 082701. [[CrossRef](#)]
219. Ryutov, D.D.; Remington, B.A. A “Perfect” Hydrodynamic Similarity and Effect of the Reynolds Number on the Global Scale Motion. *Phys. Plasmas* **2003**, *10*, 2629–2632. [[CrossRef](#)]
220. Degraeve, J.; Felici, F.; Buchli, J.; Neunert, M.; Tracey, B.; Carpanese, F.; Ewalds, T.; Hafner, R.; Abdolmaleki, A.; de las Casas, D.; et al. Magnetic Control of Tokamak Plasmas through Deep Reinforcement Learning. *Nature* **2022**, *602*, 414–419. [[CrossRef](#)]
221. Beaux, M.F.; Hass, J.; Bridges, N.; Kwon, N.H.; McIlroy, D.N. Reynolds Number Manipulation of Mean Nanowire Lengths and Nanowire Suspension Quantification. *J. Appl. Phys.* **2011**, *110*, 024313. [[CrossRef](#)]
222. Kim, Y.; Lee Chung, B.; Ma, M.; Mulder, W.J.M.; Fayad, Z.A.; Farokhzad, O.C.; Langer, R. Mass Production and Size Control of Lipid-Polymer Hybrid Nanoparticles through Controlled Microvortices. *Nano Lett.* **2012**, *12*, 3587–3591. [[CrossRef](#)] [[PubMed](#)]
223. Deepak, K.; Rathore, J.S.; Sharma, N.N. Nanorobot Propulsion Using Helical Elastic Filaments at Low Reynolds Numbers. *J. Nanotechnol. Eng. Med.* **2011**, *2*, 011009. [[CrossRef](#)]
224. Venu Vinod, A.; Sadasiva Rao, P. Microfluidics of Nanodrug Delivery: Effect of Reynolds Number Ratio and Particle Size. *Chem. Prod. Process Model.* **2011**, *6*, 32. [[CrossRef](#)]
225. Driss, Z.; Karray, S.; Damak, A.; Abid, M.S. Effect of the Reynolds Number on the Aerodynamic Characteristics of a Horizontal Axis Wind Turbine. In Proceedings of the 2012 1st International Conference on Renewable Energies and Vehicular Technology, REVET 2012, Nabeul, Tunisia, 26–28 March 2012; pp. 317–323. [[CrossRef](#)]
226. Bourhis, M.; Pereira, M.; Ravelet, F. Experimental Investigation of the Effects of the Reynolds Number on the Performance and Near Wake of a Wind Turbine. *Renew. Energy* **2023**, *209*, 63–70. [[CrossRef](#)]
227. Bachant, P.; Wosnik, M. Effects of Reynolds Number on the Energy Conversion and Near-Wake Dynamics of a High Solidity Vertical-Axis Cross-Flow Turbine. *Energies* **2016**, *9*, 73. [[CrossRef](#)]
228. Cunningham, J.B.; Lemieux, P. Study of Low Reynolds Number Effects on Small Wind Turbine Performance. In Proceedings of the AIAA SciTech Forum, San Diego, CA, USA, 3–7 January 2022. [[CrossRef](#)]
229. Burdett, T.A.; Gregg, J.A.; Van Treuren, K.W. A Numerical Study on Improving Airfoil Performance at Low Reynolds Numbers for Small-Scale Wind Turbines Using Intentional Roughness. In Proceedings of the 50th AIAA Aerospace Sciences Meeting Including the New Horizons Forum and Aerospace Exposition, Nashville, TN, USA, 9–12 January 2012. [[CrossRef](#)]
230. Mohan, M.; Talukdar, P.K.; Saha, U.K. Influence of Reynolds Number on Aerodynamic and Performance Coefficients of a Novel Parabolic-Bladed Savonius Wind Rotor. *J. Energy Resour. Technol.* **2024**, *146*, 111801. [[CrossRef](#)]
231. Javed, A.; Djidjeli, K.; Naveed, A.; Xing, J.T. Low Reynolds Number Effect on Energy Extraction Performance of Semi-Passive Flapping Foil. *J. Appl. Fluid Mech.* **2018**, *11*, 1613–1627. [[CrossRef](#)]
232. Gurka, R.; Nafi, A.S.; Weihs, D. On an Adaptation of the Reynolds Number, Applicable to Body-Caudal-Fin Aquatic Locomotion. *Front. Mar. Sci.* **2022**, *9*, 914214. [[CrossRef](#)]
233. Cohen, N.; Boyle, J.H. Swimming at Low Reynolds Number: A Beginners Guide to Undulatory Locomotion. *Contemp. Phys.* **2010**, *51*, 103–123. [[CrossRef](#)]
234. McHenry, M.J.; Azizi, E.; Strother, J.A. The Hydrodynamics of Locomotion at Intermediate Reynolds Numbers: Undulatory Swimming in Ascidian Larvae (*Botrylloides* sp.). *J. Exp. Biol.* **2003**, *206*, 327–343. [[CrossRef](#)] [[PubMed](#)]
235. Gazzola, M.; Argentina, M.; Mahadevan, L. Scaling Macroscopic Aquatic Locomotion. *Nat. Phys.* **2014**, *10*, 758–761. [[CrossRef](#)]

236. Govardhan, R.N.; Arakeri, J.H. Fluid Mechanics of Aquatic Locomotion at Large Reynolds Numbers. *J. Indian Inst. Sci.* **2011**, *91*, 329–352.
237. Webb, P.W. Simple Physical Principles and Vertebrate Aquatic Locomotion. *Integr. Comp. Biol.* **1988**, *28*, 709–725. [[CrossRef](#)]
238. Techet, A.H. Propulsive Performance of Biologically Inspired Flapping Foils at High Reynolds Numbers. *J. Exp. Biol.* **2008**, *211*, 274–279. [[CrossRef](#)] [[PubMed](#)]
239. Moslemi, A.A.; Krueger, P.S. The Effect of Reynolds Number on the Propulsive Efficiency of a Biomorphic Pulsed-Jet Underwater Vehicle. *Bioinspir. Biomim.* **2011**, *6*, 026001. [[CrossRef](#)]
240. Wu, T.Y. *Introduction to the Scaling of Aquatic Animal Locomotion*; California Institute of Technology: Pasadena, CA, USA, 1977.
241. Channouf, S.; Jami, M. Impact Dynamics of Droplets on Circular Bodies: Exploring the Influence of Wettability, Viscosity, and Body Dimensions Using the Lattice Boltzmann Method. *Phys. Fluids* **2024**, *36*, 053316. [[CrossRef](#)]
242. Lv, Q.; Li, J.; Guo, P.; Zhang, B.; Tang, P. Effect of Reynolds Number on Impact Force and Collision Process of a Low-Velocity Droplet Colliding with a Wall Carrying an Equal-Mass Deposited Droplet. *Int. J. Multiph. Flow* **2023**, *163*, 104432. [[CrossRef](#)]
243. Gordillo, L.; Sun, T.P.; Cheng, X. Dynamics of Drop Impact on Solid Surfaces: Evolution of Impact Force and Self-Similar Spreading. *J. Fluid Mech.* **2018**, *840*, 190–214. [[CrossRef](#)]
244. Tretola, G.; Vogiatzaki, K. Unveiling the Dynamics of Ultra High Velocity Droplet Impact on Solid Surfaces. *Sci. Rep.* **2022**, *12*, 7416. [[CrossRef](#)]
245. Marmanis, H.; Thoroddsen, S.T. Scaling of the Fingering Pattern of an Impacting Drop. *Phys. Fluids* **1996**, *8*, 1344–1346. [[CrossRef](#)]
246. Bolleddula, D.A.; Berchielli, A.; Aliseda, A. Impact of a Heterogeneous Liquid Droplet on a Dry Surface: Application to the Pharmaceutical Industry. *Adv. Colloid Interface Sci.* **2010**, *159*, 144–159. [[CrossRef](#)] [[PubMed](#)]
247. Chen, H.; Hugo, R.; Park, S. In-Situ Modal Response Characterization of Pipe Structures Through Reynolds Number Variation. In Proceedings of the Biennial International Pipeline Conference, IPC, Calgary, AB, Canada, 24–28 September 2018; Volume 3, p. 9. [[CrossRef](#)]
248. Bakshi, S.; Roisman, I.V.; Tropea, C. Investigations on the Impact of a Drop onto a Small Spherical Target. *Phys. Fluids* **2007**, *19*, 032102. [[CrossRef](#)]
249. Anyoji, M.; Hamada, D. High-Performance Airfoil with Low Reynolds-Number Dependence on Aerodynamic Characteristics. *Fluid Mech. Res. Int. J.* **2019**, *3*, 76–80. [[CrossRef](#)]
250. Baljé, O.E. A Study on Reynolds Number Effects in Turbomachines. *J. Eng. Power* **1964**, *86*, 227–235. [[CrossRef](#)]
251. Ivanco, T.G.; Keller, D.F.; Pinkerton, J.L. Effect of Reynolds Number and Aeroelastic Scaling Upon Launch-Vehicle Ground-Wind Loads. *J. Spacecr. Rocket.* **2024**, *61*, 1305–1312. [[CrossRef](#)]
252. Penland, J.A.; Romeo, D.J. Advances in Hypersonic Exploration Capability- Wind Tunnel to Flight Reynolds Number. *J. Aircr.* **1971**, *8*, 881–884. [[CrossRef](#)]
253. Bensignor, I.; Seth, D.; McCrink, M. Rotor Propulsion Modeling for Low Reynolds Number Flow ( $Re < 10^5$ ) for Martian Rotorcraft Flight. In Proceedings of the AIAA AVIATION 2022 Forum, Chicago, IL, USA, 27 June–1 July 2022; American Institute of Aeronautics and Astronautics: Reston, VA, USA, 2022.
254. Schneider, S.P. Laminar-Turbulent Transition on Reentry Capsules and Planetary Probes. *J. Spacecr. Rocket.* **2006**, *43*, 1153–1173. [[CrossRef](#)]
255. Purcell, E.M. Life at Low Reynolds Number. In *Physics and Our World*; World Scientific Publishing Company: London, UK, 2013; pp. 47–67. [[CrossRef](#)]
256. Gad-El Hak, M.; Bandyopadhyay, P.R. Reynolds Number Effects in Wall-Bounded Turbulent Flows. *Appl. Mech. Rev.* **1994**, *47*, 307–365. [[CrossRef](#)]
257. Donnelly, R.; Smith, M.; Swanson, C. Superfluid Wind Tunnels. *Phys. World* **1990**, *3*, 39. [[CrossRef](#)]
258. Salac, D.; Miksis, M.J. Reynolds Number Effects on Lipid Vesicles. *J. Fluid Mech.* **2012**, *711*, 122–146. [[CrossRef](#)]
259. Varela, P.; Suárez, P.; Alcántara-Ávila, F.; Miró, A.; Rabault, J.; Font, B.; García-Cuevas, L.M.; Lehmkuhl, O.; Vinuesa, R. Deep Reinforcement Learning for Flow Control Exploits Different Physics for Increasing Reynolds Number Regimes. *Actuators* **2022**, *11*, 359. [[CrossRef](#)]
260. Heuveline, V.; Wittwer, P. Exterior Flows at Low Reynolds Numbers: Concepts, Solutions, and Applications. In *Fundamental Trends in Fluid-Structure Interaction*; World Scientific Publishing Company: London, UK, 2010; pp. 77–169. [[CrossRef](#)]
261. Akhter, M.Z.; Riyadh Ali, A.; Omar, F.K. Effect of Flow Reynolds Number on the Aerodynamics of a Novel Bionic Morphing Flap. In Proceedings of the 2022 Advances in Science and Engineering Technology International Conferences, ASET 2022, Dubai, United Arab Emirates, 21–24 February 2022. [[CrossRef](#)]
262. Zheng, C.; Zhou, P.; Zhong, S.; Zhang, X. On the Cylinder Noise and Drag Reductions in Different Reynolds Number Ranges Using Surface Pattern Fabrics. *Phys. Fluids* **2023**, *35*, 035111. [[CrossRef](#)]
263. Ajayi, O.E.; Lawal, K.A.; Ukaonu, C.E.; Alabi, T.; Okoh, O.; Igbokwe, O. On the Characterisation of the Flow Regimes of Drilling Fluids. In Proceedings of the Society of Petroleum Engineers—SPE Nigeria Annual International Conference and Exhibition 2019, NAIC 2019, Lagos, Nigeria, 5–7 August 2019. [[CrossRef](#)]
264. Pavlíček, P. Local Reynolds Number. *AIP Conf. Proc.* **2019**, *2118*, 030035. [[CrossRef](#)]
265. Ghosh, B.; Kozarević, E. Identifying Explosive Behavioral Trace in the CNX Nifty Index: A Quantum Finance Approach. *Investig. Manag. Financ. Innov.* **2018**, *15*, 208–223. [[CrossRef](#)]
266. Ghosh, B.; Krishna, M.C. Econophysics Reviews. *SSRN Electron. J.* **2019**. [[CrossRef](#)]

267. Hildebrand, N.; Choudhari, M.M.; Duan, L. Effect of the Reynolds Number on the Freestream Disturbance Environment in a Mach 6 Nozzle. In Proceedings of the AIAA AVIATION 2022 Forum, Chicago, IL, USA, 27 June–1 July 2022. [\[CrossRef\]](#)
268. Silva, T.S.; Zecchetto, M.; Da Silva, C.B. The Scaling of the Turbulent/Non-Turbulent Interface at High Reynolds Numbers. *J. Fluid. Mech.* **2018**, *843*, 156–179. [\[CrossRef\]](#)
269. Yeung, P.K.; Donzis, D.A.; Sreenivasan, K.R. High-Reynolds-Number Simulation of Turbulent Mixing. *Phys. Fluids* **2005**, *17*, 081703. [\[CrossRef\]](#)
270. Ishihara, T.; Gotoh, T.; Kaneda, Y. Study of High-Reynolds Number Isotropic Turbulence by Direct Numerical Simulation. *Annu. Rev. Fluid Mech.* **2009**, *41*, 165–180. [\[CrossRef\]](#)
271. Alfonsi, G. Reynolds-Averaged Navier-Stokes Equations for Turbulence Modeling. *Appl. Mech. Rev.* **2009**, *62*, 040802. [\[CrossRef\]](#)
272. Tang, L. Reynolds-Averaged Navier-Stokes Simulation of Low-Reynolds-Number Airfoil Aerodynamics. *J. Aircr.* **2008**, *45*, 848–856. [\[CrossRef\]](#)
273. Piomelli, U. High Reynolds Number Calculations Using the Dynamic Subgrid-Scale Stress Model. *Phys. Fluids A Fluid Dyn.* **1993**, *5*, 1484–1490. [\[CrossRef\]](#)
274. Voke, P.R. Subgrid-Scale Modelling at Low Mesh Reynolds Number. *Theor. Comput. Fluid Dyn.* **1996**, *8*, 131–143. [\[CrossRef\]](#)
275. Xu, C.X.; Wang, Z.Y.; Cui, G.X.; Zhang, Z.S. Multiscale Large Eddy Simulation of Scalar Transport in Turbulent Channel Flow. In *New Trends in Fluid Mechanics Research*; Springer: Berlin/Heidelberg, Germany, 2007; pp. 111–114. [\[CrossRef\]](#)
276. Madlener, K.; Frey, B.; Ciezki, H.K. Generalized Reynolds Number for Non-Newtonian Fluids. *Prog. Propuls. Phys.* **2009**, *1*, 237–250. [\[CrossRef\]](#)
277. Foong, L.K.; Shirani, N.; Toghraie, D.; Zarringhalam, M.; Afrand, M. Numerical Simulation of Blood Flow inside an Artery under Applying Constant Heat Flux Using Newtonian and Non-Newtonian Approaches for Biomedical Engineering. *Comput. Methods Programs Biomed.* **2020**, *190*, 105375. [\[CrossRef\]](#) [\[PubMed\]](#)
278. Giesekus, H. Stoff- Und Wärmeübertragung Beim Strömen Schwach Viskoelastischer Flüssigkeiten Um Eine Rotierende Kugel. *Rheol. Acta* **1970**, *9*, 30–38. [\[CrossRef\]](#)
279. Garduño, I.E.; Tamaddon-Jahromi, H.R.; Webster, M.F. Oldroyd-B Numerical Solutions about a Rotating Sphere at Low Reynolds Number. *Rheol. Acta* **2015**, *54*, 235–251. [\[CrossRef\]](#)
280. Garduño, I.E.; Tamaddon-Jahromi, H.R.; Walters, K.; Webster, M.F. The Interpretation of a Long-Standing Rheological Flow Problem Using Computational Rheology and a PTT Constitutive Model. *J. Nonnewton Fluid Mech.* **2016**, *233*, 27–36. [\[CrossRef\]](#)
281. Chen, L.; Yang, C.; Xiao, Y.; Yan, X.; Hu, L.; Eggersdorfer, M.; Chen, D.; Weitz, D.A.; Ye, F. Microfluidics, Microfluidics, and Nanofluidics: Manipulating Fluids at Varying Length Scales. *Mater. Today Nano* **2021**, *16*, 100136. [\[CrossRef\]](#)
282. Hu, G.; Li, D. Multiscale Phenomena in Microfluidics and Nanofluidics. *Chem. Eng. Sci.* **2007**, *62*, 3443–3454. [\[CrossRef\]](#)
283. Wornom, S.; Ouvrard, H.; Salvetti, M.V.; Koobus, B.; Dervieux, A. Variational Multiscale Large-Eddy Simulations of the Flow Past a Circular Cylinder: Reynolds Number Effects. *Comput. Fluids* **2011**, *47*, 44–50. [\[CrossRef\]](#)
284. Chen, S.; Wang, M.; Xia, Z. Multiscale Fluid Mechanics and Modeling. *Procedia IUTAM* **2014**, *10*, 100–114. [\[CrossRef\]](#)
285. Ferziger, J.H.; Koseff, J.R.; Monismith, S.G. Numerical Simulation of Geophysical Turbulence. *Comput. Fluids* **2002**, *31*, 557–568. [\[CrossRef\]](#)
286. Chapman, D. *An Approximate Analytical Method for Studying Entry into Planetary Atmospheres*; Moffett Field: Mountain View, CA, USA, 1958.
287. Intrieri, P.F.; De Rose, C.E.; Kirk, D.B. Flight Characteristics of Probes in the Atmospheres of Mars, Venus and the Outer Planets. *Acta Astronaut.* **1977**, *4*, 789–799. [\[CrossRef\]](#)
288. Reeves, M.T.; Billam, T.P.; Anderson, B.P.; Bradley, A.S. Identifying a Superfluid Reynolds Number via Dynamical Similarity. *Phys. Rev. Lett.* **2015**, *114*, 155302. [\[CrossRef\]](#)
289. Takeuchi, H. Quantum Viscosity and the Reynolds Similitude of a Pure Superfluid. *Phys. Rev. B* **2024**, *109*, L020502. [\[CrossRef\]](#)
290. Barenghi, C.F. Is the Reynolds Number Infinite in Superfluid Turbulence? *Phys. D* **2008**, *237*, 2195–2202. [\[CrossRef\]](#)
291. Volovik, G.E. Classical and Quantum Regimes of Superfluid Turbulence. *JETP Lett.* **2003**, *78*, 533–537. [\[CrossRef\]](#)
292. Marusic, I.; McKeon, B.J.; Monkewitz, P.A.; Nagib, H.M.; Smits, A.J.; Sreenivasan, K.R. Wall-Bounded Turbulent Flows at High Reynolds Numbers: Recent Advances and Key Issues. *Phys. Fluids* **2010**, *22*, 065103. [\[CrossRef\]](#)
293. Dmitrenko, A.V.; Ovsyannikov, V.M. Theoretical Estimates of the Critical Reynolds Number in the Flow around the Sphere on the Basis of Theory of Stochastic Equations and Equivalence of Measures. *Fluids* **2023**, *8*, 81. [\[CrossRef\]](#)
294. Liebendorfer, A. New Theoretical Model for Effects of Reynolds Number on Laminar Boundary Layer along Ribbed Surfaces. *Scilight* **2019**, *2019*, 180004. [\[CrossRef\]](#)
295. Sanfins, G.; Anbarlooei, H.R.; Cruz, D.O.A.; Ramos, F. Complete and Incomplete Similarity for the Mean Velocity Profile of Turbulent Pipe and Channel Flows at Extreme Reynolds Number. *Phys. Fluids* **2021**, *33*, 085118. [\[CrossRef\]](#)
296. Anbarlooei, H.R.; Cruz, D.O.A.; Ramos, F. New Power-Law Scaling for Friction Factor of Extreme Reynolds Number Pipe Flows. *Phys. Fluids* **2020**, *32*, 095121. [\[CrossRef\]](#)
297. Moriconi, L.; Pereira, R.M. Statistics of Extreme Turbulent Circulation Events from Multifractality Breaking. *Phys. Rev. E* **2022**, *106*, 054121. [\[CrossRef\]](#) [\[PubMed\]](#)
298. Chini, G.P. Exact Coherent Structures at Extreme Reynolds Number. *J. Fluid Mech.* **2016**, *794*, 1–4. [\[CrossRef\]](#)
299. Klewicki, J.C.; Chini, G.P.; Gibson, J.F. Prospectus: Towards the Development of High-Fidelity Models of Wall Turbulence at Large Reynolds Number. *Philos. Trans. R. Soc. A Math. Phys. Eng. Sci.* **2017**, *375*, 20160092. [\[CrossRef\]](#) [\[PubMed\]](#)

300. Laguarda, L.; Hickel, S.; Schrijer, F.F.J.; van Oudheusden, B.W. Reynolds Number Effects in Shock-Wave/Turbulent Boundary-Layer Interactions. *J. Fluid Mech.* **2024**, *989*, A20. [[CrossRef](#)]
301. Ashoor, M.; Khorshidi, A.; Pirouzi, A.; Abdollahi, A.; Mohsenzadeh, M.; Barzi, S.M.Z. Estimation of Reynolds Number on Microvasculature Capillary Bed Using Diffusion and Perfusion MRI: The Theoretical and Experimental Investigations. *Eur. Phys. J. Plus* **2021**, *136*, 152. [[CrossRef](#)]
302. Martínez, I.A.; Roldán, E.; Dinis, L.; Petrov, D.; Parrondo, J.M.R.; Rica, R.A. Brownian Carnot Engine. *Nat. Phys.* **2015**, *12*, 67–70. [[CrossRef](#)] [[PubMed](#)]
303. Jayapregasham, S. *Effect of Varying Reynolds Number On The Aerodynamic Design of Lifting Surfaces*; Embry-Riddle Aeronautical University: Daytona Beach, FL, USA, 2021.
304. Dimotakis, P.E. Turbulent Mixing. *Annu. Rev. Fluid Mech.* **2005**, *37*, 329–356. [[CrossRef](#)]
305. Hanjalić, K. Will RANS Survive LES? A View of Perspectives. In Proceedings of the ASME Heat Transfer/Fluids Engineering Summer Conference 2004, HT/FED 2004, Charlotte, NC, USA, 1–15 July 2004; Volume 2A, pp. 715–725. [[CrossRef](#)]
306. Ericsson, L.; Reding, J. Reynolds Number Criticality in Dynamic Tests. In Proceedings of the 16th Aerospace Sciences Meeting, Huntsville, AL, USA, 16–18 January 1978; American Institute of Aeronautics and Astronautics: Reston, VA, USA, 1978.
307. Quinn, H.M. A Fluid Dynamic Development Like None Other. *Eur. J. Appl. Sci.* **2023**, *11*, 407–429. [[CrossRef](#)]
308. Das, R.; Girimaji, S.S. On the Reynolds Number Dependence of Velocity-Gradient Structure and Dynamics. *J. Fluid Mech.* **2019**, *861*, 163–179. [[CrossRef](#)]
309. Jones, W.P.; Launder, B.E. The Calculation of Low-Reynolds-Number Phenomena with a Two-Equation Model of Turbulence. *Int. J. Heat Mass. Transf.* **1973**, *16*, 1119–1130. [[CrossRef](#)]
310. Brodkey, R.S. Limitations on a Generalized Velocity Distribution. *AIChE J.* **1963**, *9*, 448–451. [[CrossRef](#)]
311. Heller, V. Scale effects in physical hydraulic engineering models. *J. Hydraul. Res.* **2012**, *50*, 244–246. [[CrossRef](#)]
312. Patel, V.C. Perspective: Flow at High Reynolds Number and Over Rough Surfaces—Achilles Heel of CFD. *J. Fluids Eng.* **1998**, *120*, 434–444. [[CrossRef](#)]
313. Heller, V. Self-Similarity and Reynolds Number Invariance in Froude Modelling. *J. Hydraul. Res.* **2017**, *55*, 293–309. [[CrossRef](#)]
314. Avila, M.; Barkley, D.; Hof, B. Transition to Turbulence in Pipe Flow. *Annu. Rev. Fluid Mech.* **2023**, *55*, 575–602. [[CrossRef](#)]
315. Chhabra, R.P.; Richardson, J.F. *Non-Newtonian Flow in the Process Industries: Fundamentals and Engineering Applications*; Butterworth-Heinemann: Oxford, UK, 2004; ISBN 9780750637701.
316. Yalin, M.S. *Theory of Hydraulic Models*; Macmillan: London, UK, 1971. [[CrossRef](#)]
317. Brennen, C.E. *Fundamentals of Multiphase Flow*; Cambridge University Press: London, UK, 2005. [[CrossRef](#)]
318. Anderson, J.D.; Cadou, C. *Fundamentals of Aerodynamics*, 7th ed.; McGraw Hill LLC: New York, NY, USA, 2024; p. 1142. ISBN 9781264151929.
319. Poelma, C. Ultrasound Imaging Velocimetry: A Review. *Exp. Fluids* **2016**, *58*, 3. [[CrossRef](#)]
320. Karniadakis, G.; Beskok, A.; Aluru, N. *Microflows and Nanoflows*; Antman, S.S., Marsden, J.E., Sirovich, L., Eds.; Interdisciplinary Applied Mathematics; Springer: New York, NY, USA, 2005; Volume 29, ISBN 0-387-22197-2.
321. Ewoldt, R.H.; Johnston, M.T.; Caretta, L.M. *Experimental Challenges of Shear Rheology: How to Avoid Bad Data*; Springer: New York, NY, USA, 2015; pp. 207–241.
322. Sreenivasan, K.R. Turbulent Mixing: A Perspective. *Proc. Natl. Acad. Sci. USA* **2019**, *116*, 18175–18183. [[CrossRef](#)] [[PubMed](#)]
323. Lee, M.; Moser, R.D. Direct Numerical Simulation of Turbulent Channel Flow up To. *J. Fluid Mech.* **2015**, *774*, 395–415. [[CrossRef](#)]
324. Balachandar, S.; Eaton, J.K. Turbulent Dispersed Multiphase Flow. *Annu. Rev. Fluid Mech.* **2010**, *42*, 111–133. [[CrossRef](#)]
325. Chabannes, V.; Prud’Homme, C.; Szopos, M.; Tarabay, R. High Order Finite Element Simulations for Fluid Dynamics Validated by Experimental Data from the Fda Benchmark Nozzle Model. *Comput. Methods Biomech. Biomed. Engin* **2017**, *20*, 139–140.
326. Marchetti, M.C.; Joanny, J.F.; Ramaswamy, S.; Liverpool, T.B.; Prost, J.; Rao, M.; Simha, R.A. Hydrodynamics of Soft Active Matter. *Rev. Mod. Phys.* **2013**, *85*, 1143–1189. [[CrossRef](#)]
327. Westerweel, J.; Elsinga, G.E.; Adrian, R.J. Particle Image Velocimetry for Complex and Turbulent Flows. *Annu. Rev. Fluid Mech.* **2013**, *45*, 409–436. [[CrossRef](#)]
328. Wang, T. A Brief Review on Wind Turbine Aerodynamics. *Theor. Appl. Mech. Lett.* **2012**, *2*, 062001. [[CrossRef](#)]
329. Snel, H. Review of Aerodynamics for Wind Turbines. *Wind Energy* **2003**, *6*, 203–211. [[CrossRef](#)]
330. Trivedi, C.; Gandhi, B.; Michel, C.J. Effect of Transients on Francis Turbine Runner Life: A Review. *J. Hydraul. Res.* **2013**, *51*, 121–132. [[CrossRef](#)]
331. Bahaj, A.S. Generating Electricity from the Oceans. *Renew. Sustain. Energy Rev.* **2011**, *15*, 3399–3416. [[CrossRef](#)]
332. Nalla, G.; Shook, G.M.; Mines, G.L.; Bloomfield, K.K. Parametric Sensitivity Study of Operating and Design Variables in Wellbore Heat Exchangers. *Geothermics* **2005**, *34*, 330–346. [[CrossRef](#)]
333. Bridgwater, A.V. Review of Fast Pyrolysis of Biomass and Product Upgrading. *Biomass Bioenergy* **2012**, *38*, 68–94. [[CrossRef](#)]
334. Falcão, A.F.d.O. Wave Energy Utilization: A Review of the Technologies. *Renew. Sustain. Energy Rev.* **2010**, *14*, 899–918. [[CrossRef](#)]
335. Williamson, S.J.; Stark, B.H.; Booker, J.D. Low Head Pico Hydro Turbine Selection Using a Multi-Criteria Analysis. *Renew. Energy* **2014**, *61*, 43–50. [[CrossRef](#)]
336. Anderson, J.D. *Hypersonic and High-Temperature Gas Dynamics*, 3rd ed.; AIAA Education Series: Las Vegas, NV, USA, 2019. [[CrossRef](#)]
337. Gnoffo, P.A. Planetary-Entry Gas Dynamics. *Annu. Rev. Fluid Mech.* **1999**, *31*, 459–494. [[CrossRef](#)]

338. Sutton, G.P.; Biblarz, O. *Rocket Propulsion Elements*, 9th ed.; Wiley: Hoboken, NJ, USA, 2016; Volume 59, ISBN 978-1-118-75365-1.
339. Braun, R.D.; Manning, R.M. Mars Exploration Entry, Descent, and Landing Challenges. *J. Spacecr. Rocket.* **2007**, *44*, 310–323. [[CrossRef](#)]
340. Goebel, D.M.; Katz, I. *Fundamentals of Electric Propulsion: Ion and Hall Thrusters*; John Wiley & Sons: Hoboken, NJ, USA, 2008; pp. 1–507. [[CrossRef](#)]
341. Marren, D.; Lu, F. *Advanced Hypersonic Test Facilities*; American Institute of Aeronautics and Astronautics: Reston, VA, USA, 2002.
342. McNamara, J.J.; Friedmann, P.P. Aeroelastic and Aerothermoelastic Analysis in Hypersonic Flow: Past, Present, and Future. *AIAA J.* **2011**, *49*, 1089–1122. [[CrossRef](#)]
343. Boyd, I.D.; Schwartzentruber, T.E. *Nonequilibrium Gas Dynamics and Molecular Simulation*; Cambridge University Press: Cambridge, UK, 2017; pp. 1–360. [[CrossRef](#)]
344. Read, P.L.; Lewis, S.R. *The Martian Climate Revisited: Atmosphere and Environment of a Desert Planet*; Springer: Berlin/Heidelberg, Germany, 2004; ISBN 9783540407430.
345. Laub, B.; Venkatapathy, E.; Laub, B.; Venkatapathy, E. Thermal Protection System Technology and Facility Needs for Demanding Future Planetary Missions. *ESASP* **2004**, *544*, 239–247.
346. Lani, A.; Sharma, V.; Giangaspero, V.F.; Poedts, S.; Viladegut, A.; Chazot, O.; Giacomelli, J.; Oswald, J.; Behnke, A.; Pagan, A.S.; et al. A Magnetohydrodynamic Enhanced Entry System for Space Transportation: MEESS. *J. Space Saf. Eng.* **2023**, *10*, 27–34. [[CrossRef](#)]
347. Samaha, M.A.; Tafreshi, H.V.; Gad-el-Hak, M. Superhydrophobic Surfaces: From the Lotus Leaf to the Submarine. *Comptes Rendus Méc.* **2012**, *340*, 18–34. [[CrossRef](#)]
348. Mahian, O.; Kolsi, L.; Amani, M.; Estellé, P.; Ahmadi, G.; Kleinstreuer, C.; Marshall, J.S.; Siavashi, M.; Taylor, R.A.; Niazmand, H.; et al. Recent Advances in Modeling and Simulation of Nanofluid Flows-Part I: Fundamentals and Theory. *Phys. Rep.* **2019**, *790*, 1–48. [[CrossRef](#)]
349. Cushman, J.H. *The Physics of Fluids in Hierarchical Porous Media: Angstroms to Miles*; Theory and Applications of Transport in Porous Media; Springer: Dordrecht, The Netherlands, 1997; Volume 10, ISBN 978-90-481-4909-4.
350. Lejars, M.; Margailan, A.; Bressy, C. Fouling Release Coatings: A Nontoxic Alternative to Biocidal Antifouling Coatings. *Chem. Rev.* **2012**, *112*, 4347–4390. [[CrossRef](#)]
351. Thévenot, J.; Oliveira, H.; Sandre, O.; Lecommandoux, S. Magnetic Responsive Polymer Composite Materials. *Chem. Soc. Rev.* **2013**, *42*, 7099–7116. [[CrossRef](#)]
352. Ceccio, S.L. Friction Drag Reduction of External Flows with Bubble and Gas Injection. *Annu. Rev. Fluid Mech.* **2010**, *42*, 183–203. [[CrossRef](#)]
353. Saidur, R.; Leong, K.Y.; Mohammed, H.A. A Review on Applications and Challenges of Nanofluids. *Renew. Sustain. Energy Rev.* **2011**, *15*, 1646–1668. [[CrossRef](#)]
354. Yim, E.K.F.; Sheetz, M.P. Force-Dependent Cell Signaling in Stem Cell Differentiation. *Stem Cell Res. Ther.* **2012**, *3*, 41. [[CrossRef](#)]
355. Bhushan, B.; Jung, Y.C. Natural and Biomimetic Artificial Surfaces for Superhydrophobicity, Self-Cleaning, Low Adhesion, and Drag Reduction. *Prog. Mater. Sci.* **2011**, *56*, 1–108. [[CrossRef](#)]
356. Cattafesta, L.N.; Sheplak, M. Actuators for Active Flow Control. *Annu. Rev. Fluid Mech.* **2011**, *43*, 247–272. [[CrossRef](#)]
357. D’Alessandro, D.M.; Smit, B.; Long, J.R. Carbon Dioxide Capture: Prospects for New Materials. *Angew. Chem. Int. Ed.* **2010**, *49*, 6058–6082. [[CrossRef](#)] [[PubMed](#)]

**Disclaimer/Publisher’s Note:** The statements, opinions and data contained in all publications are solely those of the individual author(s) and contributor(s) and not of MDPI and/or the editor(s). MDPI and/or the editor(s) disclaim responsibility for any injury to people or property resulting from any ideas, methods, instructions or products referred to in the content.